

Prediction of potential drug interactions between repurposed COVID-19 and antitubercular drugs: an integrational approach of drug information software and computational techniques data

Levin Thomas, Sumit Raosaheb Birangal, Rajdeep Ray, Sonal Sekhar Miraj , Murali Munisamy, Muralidhar Varma, Chidananda Sanju S.V., Mithu Banerjee, Gautham G. Shenoy and Mahadev Rao 

Abstract

Introduction: Tuberculosis is a major respiratory disease globally with a higher prevalence in Asian and African countries than rest of the world. With a larger population of tuberculosis patients anticipated to be co-infected with COVID-19 infection, an ongoing pandemic, identifying, preventing and managing drug–drug interactions is inevitable for maximizing patient benefits for the current repurposed COVID-19 and antitubercular drugs.

Methods: We assessed the potential drug–drug interactions between repurposed COVID-19 drugs and antitubercular drugs using the drug interaction checker of IBM Micromedex®. Extensive computational studies were performed at a molecular level to validate and understand the drug–drug interactions found from the Micromedex drug interaction checker database at a molecular level. The integrated knowledge derived from Micromedex and computational data was collated and curated for predicting potential drug–drug interactions between repurposed COVID-19 and antitubercular drugs.

Results: A total of 91 potential drug–drug interactions along with their severity and level of documentation were identified from Micromedex between repurposed COVID-19 drugs and antitubercular drugs. We identified 47 pharmacodynamic, 42 pharmacokinetic and 2 unknown DDIs. The majority of our molecular modelling results were in line with drug–drug interaction data obtained from the drug information software. QT prolongation was identified as the most common type of pharmacodynamic drug–drug interaction, whereas drug–drug interactions associated with cytochrome P450 3A4 (CYP3A4) and P-glycoprotein (P-gp) inhibition and induction were identified as the frequent pharmacokinetic drug–drug interactions. The results suggest antitubercular drugs, particularly rifampin and second-line agents, warrant high alert and monitoring while prescribing with the repurposed COVID-19 drugs.

Conclusion: Predicting these potential drug–drug interactions, particularly related to CYP3A4, P-gp and the human Ether-à-go-go-Related Gene proteins, could be used in clinical settings for screening and management of drug–drug interactions for delivering safer chemotherapeutic tuberculosis and COVID-19 care. The current study provides an initial propulsion for further well-designed pharmacokinetic-pharmacodynamic-based drug–drug interaction studies.

Ther Adv Drug Saf

2021, Vol. 12: 1–29

DOI: 10.1177/
20420986211041277

© The Author(s), 2021.
Article reuse guidelines:
sagepub.com/journals-
permissions

Correspondence to:

Mahadev Rao
Professor and Head,
Department of Pharmacy
Practice, Coordinator,
Centre for Translational
Research, Manipal
College of Pharmaceutical
Sciences, Manipal
Academy of Higher
Education (MAHE), Manipal
576104, Karnataka, India.
mahadev.rao@manipal.edu

Levin Thomas
Sonal Sekhar Miraj
Murali Munisamy

Department of Pharmacy
Practice, Manipal College
of Pharmaceutical
Sciences, Manipal
Academy of Higher
Education, Manipal, India

Sumit Raosaheb Birangal
Rajdeep Ray

Gautham G. Shenoy
Department of
Pharmaceutical
Chemistry, Manipal
College of Pharmaceutical
Sciences, Manipal
Academy of Higher
Education, Manipal, India

Muralidhar Varma
Department of Infectious
Diseases, Kasturba
Medical College, Manipal
Academy of Higher
Education, Manipal, India

Chidananda Sanju S.V.
District Tuberculosis
Control Office, Ajjarakad,
Udupi, Karnataka, India

Mithu Banerjee
Department of
Biochemistry, All India
Institute of Medical
Sciences, Jodhpur,
Rajasthan, India

Plain Language Summary

Introduction: Tuberculosis is a major respiratory disease globally with a higher prevalence in Asian and African countries than rest of the world. With a larger population of tuberculosis

patients predicted to be infected with COVID-19 during this period, there is a higher risk for the occurrence of medication interactions between the medicines used for COVID-19 and tuberculosis. Hence, identifying and managing these interactions is vital to ensure the safety of patients undergoing COVID-19 and tuberculosis treatment simultaneously.

Methods: We studied the major medication interactions that could likely happen between the various medicines that are currently given for COVID-19 and tuberculosis treatment using the medication interaction checker of a drug information software (Micromedex®). In addition, thorough molecular modelling was done to confirm and understand the interactions found from the medication interaction checker database using specific docking software. Molecular docking is a method that predicts the preferred orientation of one medicine molecule to a second molecule, when bound to each other to form a stable complex. Knowledge of the preferred orientation may be used to determine the strength of association or binding affinity between two medicines using scoring functions to determine the extent of the interactions between medicines. The combined knowledge from Micromedex and molecular modelling data was used to properly predict the potential medicine interactions between currently used COVID-19 and antitubercular medicines.

Results: We found a total of 91 medication interactions from Micromedex. Majority of our molecular modelling findings matched with the interaction information obtained from the drug information software. QT prolongation, an abnormal heartbeat, was identified as one of the most common interactions. Our findings suggest that antitubercular medicines, mainly rifampin and second-line agents, suggest high alert and scrutiny while prescribing with the repurposed COVID-19 medicines.

Conclusion: Our current study highlights the need for further well-designed studies confirming the current information for recommending safe prescribing in patients with both infections.

Keywords: antitubercular drugs, drug–drug interactions, molecular docking, QT prolongation, repurposed COVID-19 drugs

Received: 3 December 2020; revised manuscript accepted: 24 July 2021.

Introduction

Tuberculosis (TB) is a major respiratory disease occurring globally, particularly in the WHO (World Health Organization) regions of South-East Asia (44%), Africa (25%) and Western Pacific (18%).^{1,2} The countries with high incidences of TB include India (26%), Indonesia (8.5%), China (8.4%), Philippines (6.0%), Pakistan (5.7%), Nigeria (4.4%), Bangladesh (3.6%) and South Africa (3.6%), which account for two-thirds of the total global TB incidences in 2019.² The global impact of Coronavirus disease-19 (COVID-19) on TB services has shown a reduction in the detection and diagnosis of TB worldwide. Moreover, there is a patient delay before the first presentation to TB care and decreased patient treatment initiation rates compared with pre-pandemic levels. These could lead to increased deaths due to TB in settings with a high TB burden.³ A modelling analysis developed

by Stop TB Partnership in collaboration with Imperial College, Avenir Health, Johns Hopkins University and United States Agency for International Development (USAID) has projected that the COVID-19 pandemic could increase by 6.3 million TB cases and 1.4 million TB deaths globally between 2020 and 2025.⁴ COVID-19 pandemic is projected to cause severe adverse impacts on poverty levels in developing countries. As poverty is a significant risk factor for the development of TB, there is an expected anticipation for a higher incidence of TB during this COVID-19 pandemic era.^{5–7} Currently, there is a paucity of data on the prevalence of TB among COVID-19 patients. TB infection has been found to increase the susceptibility, severity and mortality related to COVID-19.^{8,9} COVID-19 could occur before, simultaneously, or after the diagnosis of TB. A study with 49 COVID-19 patients from 26 centres of 8 countries reported

that 26 (53.0%) had TB before COVID-19, 14 (28.5%) had COVID-19 first and 9 (18.3%) had both diseases diagnosed within the same week (4 on the same day).¹⁰

Drug–drug interactions (DDIs) represent an austere and ubiquitous problem in patient safety, especially with geriatrics and patients on polypharmacy. Indeed, DDIs are culpable for a significant proportion of adverse drug reactions, hospital admissions, healthcare expenditures, morbidities and mortalities.^{11–15} Repurposed COVID-19 drugs have been reported to interact with drugs used in the management of other diseases.^{16,17} DDIs screening software has emerged to be an important tool for identifying and managing DDIs for clinicians, pharmacists and other healthcare providers. Micromedex is a widely used software in clinical practice for the identification of DDIs. Micromedex provides information regarding severity (contraindicated, major, moderate, minor and unknown), level of evidence (excellent, good, fair, unknown), clinical consequence, underlying mechanism, clinical management and onset of the adverse outcome (either rapid or delayed) of the DDIs.^{18,19}

DDIs are identified by various approaches such as *in silico*, *in vitro* and *in vivo* experiments. *In vitro* and *in vivo* methods are laborious and expensive. However, *in silico* modelling approaches have become robust means for examining hypotheses and understanding mechanisms related to DDIs in health research. The optimality and cost-effectiveness give an extra edge to *in silico* modelling.^{20,21} Hence, combining the data derived from DDI checker software and *in silico* computational methods are expected to provide a more comprehensive picture of the prediction of potential DDIs associated with antitubercular drugs and repurposed COVID-19 drugs.

TB treatment regimens are characterized by multidrug combinations and a longer duration of use.²² Several drugs have been reported as substrates, inhibitors and inducers for CYP3A4 and P-gp.^{23,24} CYP3A4 and P-gp are reckoned to be key molecular targets related to DDIs occurring with TB treatment.^{25,26} Hence, there is an increased potential for CYP3A4 and P-gp-based DDIs between antitubercular drugs and repurposed COVID-19 drugs. QT prolongation is also a key feature of many second-line antitubercular

drugs and repurposed COVID-19 drugs.^{27–30} The hERG is a gene that encodes for the pore-forming subunit of a delayed rectifier voltage gated K⁺ (VGK) channel, which is variously referred to as Kv11.1, I_{Kr} or as hERG. This ion channel plays an important role in the repolarization phase of the cardiac action potential by mediating the rapid component of cardiac delayed rectifier K⁺ current.^{31,32} The most common mechanism of drug-induced QT prolongation is due to hERG inhibition.^{33,34} Several antitubercular agents and repurposed COVID-19 drugs have been reported to inhibit hERG and result in QT interval prolongation.^{35–38} Hence, there is an increased potential for DDIs due to QT prolongation. This could be expected when antitubercular drugs and repurposed COVID-19 drugs with a potential for inhibition of hERG are used concomitantly. Hence, predicting these potential DDIs related to induction or inhibition of CYP3A4, P-gp and hERG in TB patients co-infected with COVID-19 could help deliver safe chemotherapeutic TB and COVID-19 care for better clinical outcomes.

With a larger population of TB patients anticipated to be co-infected with COVID-19, it may be imperative to assess the potential DDIs occurring with the antitubercular drugs with the repurposed COVID-19 drugs. To our knowledge, no studies have reported a comprehensive drug information database and molecular docking integrated data on DDIs between antitubercular drugs and repurposed COVID-19 drugs till the date. In this scenario, we assessed the potential DDIs between the repurposed COVID-19 drugs and antitubercular drugs using the drug interaction checker of IBM Micromedex®. In addition, relevant literature was extracted from PubMed and Google Scholar for gathering information regarding the mechanism of DDIs found from the drug interaction checker of Micromedex. We excluded non-scientific commentaries and only English literature were included in the study. Extensive computational studies were performed to validate and understand the DDIs found from the Micromedex drug interaction checker database at a molecular level. The information derived from this integrated data is collated and curated for providing an easy and clear picture to clinicians, nurses and pharmacists for improved identification, detection and management of DDIs of antitubercular drugs with repurposed COVID-19 drugs.

Methodology

Step 1: identifying repurposed COVID-19 drugs and antitubercular drugs for DDI assessment

The repurposed COVID-19 drugs were identified from the medications list of American Society of Health-System Pharmacists (ASHP; <https://www.ashp.org/-/media/8CA43C674C6D4335B6A19852843C4052.ashx>).³⁹ We have included repurposed drugs used as antiviral, supportive and other agents for the management of COVID-19. The final consensus list of drugs included for the final search for DDIs in the Micromedex® software was decided by a multidisciplinary and multi-institutional team comprising infectious diseases/COVID-19-treating physician, TB physician specialist, clinical pharmacist, clinical researcher, basic scientist, medicinal chemists, and medical and pharmacy academicians. We excluded COVID-19 convalescent plasma therapy from our list. The repurposed COVID-19 drugs, favipiravir, umifenovir and etesevimab, were not found in the search list of drug interaction checker of Micromedex. The potential DDIs of the repurposed COVID-19 drugs were assessed with the following antitubercular drugs: isoniazid, rifampin, pyrazinamide, ethambutol, streptomycin, amikacin, kanamycin, capreomycin, clarithromycin, levofloxacin, moxifloxacin, ofloxacin, cycloserine, amoxicillin-clavulanate, ethionamide, imipenem-cilastatin, linezolid, clofazimine, delamanid, bedaquiline and pretomanid.

Step 2: searching for DDIs in Micromedex® software

We searched to identify potential DDIs between antitubercular drugs and repurposed COVID-19 drugs by inputting all the generic names of the drugs into the drug interaction checker of IBM Micromedex®. The severity of the potential DDIs from Micromedex was classified into five groups: contraindicated, major, moderate, minor and none. All potential DDIs were collected from the Micromedex® till 24 March 2021.

Step 3: induced-fit docking (IFD) and binding free energy calculation

The protein crystal structure was downloaded from the Protein Data Bank (PDB).⁴⁰ In the crystal structures of human CYP3A4 (PDB ID: 6MA7), the active site cavities are much larger.

They are located near haem iron, allowing these enzymes to accommodate substrates or inhibitors of diverse size.⁴¹ Since the human protein structure is not available for P-gp protein, the amino acid protein sequence for human P-gp protein was obtained from the FASTA sequences from the Uniport database. For this, id P08183 and references protein (PDB ID: 3G60) in complex with the inhibitor was selected for generating a homology model. hERG protein crystal structure was downloaded from the well-established homology database of Schrodinger.⁴² The crystal structure of the protein was optimized using the Protein Preparation Wizard module of Schrodinger 2021-1. Pre-processing of the protein was achieved by assigning bond order, hydrogen addition and disulphide treatment. All the water molecules beyond 5 Å from the hetero groups were removed. Hydrogen bonds were assigned, and the orientations of the remaining water molecules were rectified. Finally, the energy of the protein structure was optimized to root mean square deviation (RMSD) of 0.30 Å by using OPLS4 force field at pH 7.4. The co-crystallized ligand was retained using default parameters in the prepared protein and was further used for grid construction.

As there was no bound ligand in the case of hERG protein and P-gp protein, site map analysis was performed using the site map analysis module to identify top-ranked receptor binding sites of the enzymes. Site maps with a site score of more than 1.15 were taken for grid generation for docking study.⁴³ After extra precision docking protocol, compounds with better docking score and pose were selected for induced fit docking with extended sampling protocol (generates up to 80 poses using automatic docking protocol). This IFD output pose was taken further for the analyses of binding energy using MM-GBSA. The purpose of this MM-GBSA is to facilitate the calculation of binding free energy using ligand binding energies and ligand strain energies.

The binding energy is calculated according to the equation:

$$\text{DG bind} = \text{Energy}_{\text{complex}} (\text{minimized}) - \text{Energy}_{\text{ligand}} (\text{minimized}) - \text{Energy}_{\text{receptor}} (\text{minimized})$$

Energy properties are calculated for the complex (E_{complex}), the ligand (E_{ligand}) and the receptor (E_{receptor}), and strain energies can be calculated for the ligand and the receptor.

We propose that most of the interactions occurring between repurposed COVID-19 drugs and antitubercular drugs are due to synergistic inhibition of hERG protein (pharmacodynamic interaction resulting in QT prolongation) or due to inhibition of CYP3A4 and P-gp (pharmacokinetic interaction leading to alteration of drug levels). Information about each drug and its role in inhibiting CYP is taken from literature and extensive computational studies are performed to validate and understand the interactions at a molecular level. The computational studies also assessed the possibility of two drugs interacting together with hERG's binding pocket.

Extensive induced-fit docking was performed for each drug on each of the target proteins viz. CYP3A4, hERG and P-gp. Binding free energy was calculated for each of the generated poses in IFD for each drug. A scoring method is then applied to calculate the net dG bind (N.S) where:

$$\text{Net Score (N.S)} = \frac{\text{A.S} \times 80 + \text{T.S}}{4}, \text{ where A.S} = \frac{\text{T.S}}{\text{N}}$$

A.S = average score; T.S (total score) = sum of dG bind (from all poses) and N = total number of poses.

For simultaneous docking studies of two molecules inside the hERG binding pocket, a single molecule was initially docked and a sitemap was run to generate the binding pocket with the first molecule and the second molecule then docked on the generated site (Table 2). Again, this step was repeated with the second molecule from step one being docked first and the first molecule docked after that (on the generated site).

Step 4: categorizing the drugs based on QT prolongation drug risk assessment

For an individual QT prolongation drug risk assessment, we have categorized the QT-prolonging drugs into four categories as per the Arizona Center for Education and Research on Therapeutics (AZCERT) classification.⁴⁴

AZCERT now maintains the Web-based lists of drugs that have a risk of QT prolongation and Torsades de Pointes (TdP). The lists are now available on the CredibleMeds Website.⁴⁵ As per the website, the drugs were categorized into:

1. Known Risk of TdP – These drugs prolong the QT interval and are clearly associated with a known risk of TdP, even when taken as recommended.
2. Possible Risk of TdP – These drugs can cause QT prolongation but currently lack evidence for a risk of TdP when taken as recommended.
3. Conditional Risk of TdP – These drugs are associated with TdP but only under certain conditions of their use (e.g. excessive dose, in patients with conditions such as hypokalemia, or when taken with interacting drugs) OR by creating conditions that facilitate or induce TdP (e.g. by inhibiting the metabolism of a QT-prolonging drug or by causing an electrolyte disturbance that induces TdP).
4. Drugs to Avoid in Congenital Long QT Syndrome (cLQTS) – These drugs pose a high risk of TdP for patients with cLQTS. They include all those in the above three categories PLUS additional drugs that do not prolong the QT interval *per se* but have a special risk (SR) because of their other actions.

Results

A total of 91 potential DDIs along with their severity and the level of documentation were identified from Micromedex between repurposed COVID-19 drugs and antitubercular drugs, as shown in Figure 1. There were 47 pharmacodynamic DDIs, 42 pharmacokinetic DDIs and 2 unknown DDIs. We identified 4 contraindicated, 65 major, 21 moderate and 1 minor DDI based on the severity of interaction. Based on the level of documentation, there were 21 DDIs with excellent documentation, whereas 25 and 45 DDIs had good and fair level of documentation, respectively.

The net binding energy of individual repurposed COVID-19 drugs and antitubercular drugs with hERG, CYP3A4 and P-gp are shown in Table 1.

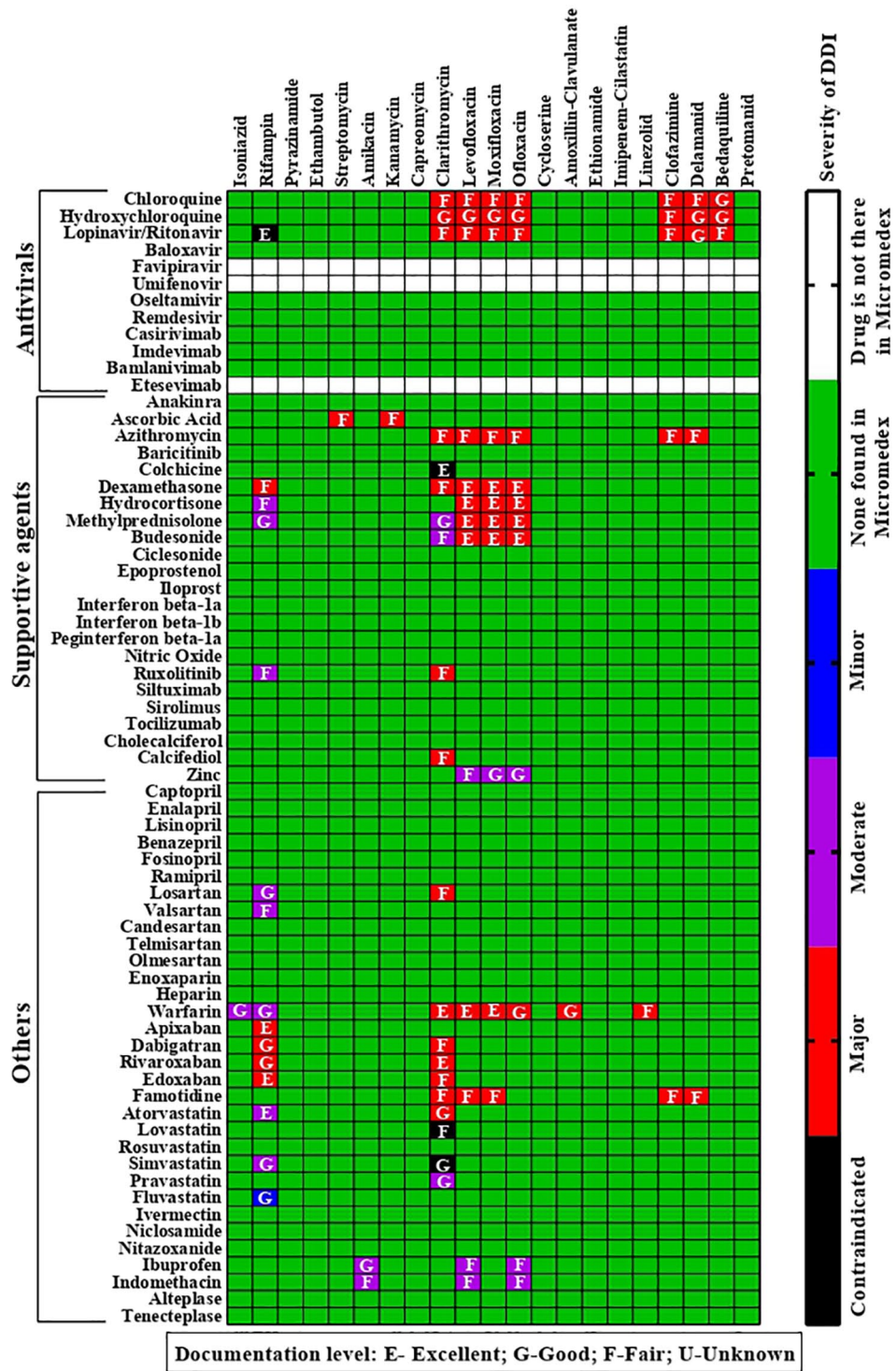


Figure 1. DDIs, along with the severity and level of documentation between repurposed COVID-19 drugs and with antitubercular drugs.

Table 1. Net binding energy of individual repurposed COVID-19 drugs and antitubercular drugs with hERG, CYP3A4 and P-gp.

	hERG	CYP3A4	P-gp
Anti TB drugs			
Isoniazid	-902.98	-1081.08	-1145.59
Rifampin	ND	ND	ND
Pyrazinamide	-861.68	-925.48	-972.66
Ethambutol	-1588.08	-1592.72	-1442.90
Streptomycin	-2137.80	-1765.55	-2000.11
Amikacin	-1496.70	-1810.30	-1769.56
Kanamycin	-1609.73	-1542.52	-1888.22
Capreomycin	-1555.68	-1487.74	-2324.40
Clarithromycin	ND	ND	ND
Levofloxacin	-1237.51	-853.37	-1653.33
Moxifloxacin	-1108.22	-882.07	-1470.86
Ofloxacin	-1244.45	-853.37	-1658.35
Cycloserine	-616.41	-822.58	-818.53
Amoxillin-Clavulanate	-1445.10	-1397.00	-1398.21
Ethionamide	-1114.50	-1215.97	-1253.72
Imipenem-Cilastatin	-810.39	-909.21	-988.20
Linezolid	-2247.39	-2402.67	-2034.76
Clofazimine	-2698.49	-2602.84	-2943.46
Delamanid	-1667.82	-1520.57	-2505.75
Bedaquiline	-1717.55	-1597.47	-2141.56
Pretomanid	-1255.58	-1666.77	-1837.87
Antivirals			
Chloroquine	-1662.35	-1277.56	-1965.43
Hydroxychloroquine	-1803.59	-1572.29	-2148.34
Ritonavir	-1298.24	-1379.59	-2095.04
Lopinavir	-1451.95	-1067.50	-1735.14
Baloxavir	-1960.16	-2863.52	-2410.27
Favipiravir	-93.69	-317.02	-636.90
Umifenovir	-1703.96	-2540.58	-2364.29
Osetamivir	-1092.98	-690.94	-1510.99
Remdesivir	-1636.25	-1387.87	-2687.21
Casirivimab	ND	ND	ND
Imdevimab	ND	ND	ND
Bamlanivimab	ND	ND	ND

(continued)

Table 1. (continued)

		hERG	CYP3A4	P-gp
	Etesevimab	ND	ND	ND
Supportive agents	Anakinra	-1690.32	-2539.57	-2698.97
	Ascorbic Acid	-779.52	-760.75	-920.86
	Azithromycin	ND	ND	ND
	Baricitinib	-1725.16	-2751.06	-2471.25
	Colchicine	-1749.96	-2537.80	-2159.07
	Dexamethasone	ND	ND	ND
	Hydrocortisone	-1692.41	-2377.34	-2846.07
	Methylprednisolone	-1913.82	-2832.10	-2683.53
	Budesonide	-2403.70	-3169.24	-3141.02
	Ciclesonide	-2713.36	-3430.60	-3854.40
	Epoprostenol	-2175.24	-3068.03	-2932.27
	Iloprost	-2370.94	-3027.87	-3107.70
	Interferon beta-1a	ND	ND	ND
	Interferon beta-1b	ND	ND	ND
Peginterferon beta-1a	ND	ND	ND	
Nitric Oxide	ND	ND	ND	
Ruxolitinib	-1875.90	-2339.74	-1647.90	
Siltuximab	ND	ND	ND	
Sirolimus	-2262.86	ND	ND	
Tocilizumab	ND	ND	ND	
Cholecalciferol	-2157.42	-3257.02	-3268.80	
Calcifediol	-2720.76	-3982.01	-3379.04	
Zinc	ND	ND	ND	
Others	Captopril	-1158.88	-1056.72	-1299.05
	Enalapril	-1503.65	-2010.73	-1958.30
	Lisinopril	-901.36	-2159.75	-1503.84
	Benazepril	-1580.24	-2006.81	-2379.72
	Fosinopril	-1705.12	-2529.65	-3123.15
	Ramipril	-1595.66	-2057.04	-2245.21
	Losartan	-1977.48	-2452.40	-2296.83
	Valsartan	-1100.99	-1510.92	-1861.07
Candesartan	-1108.05	-1639.74	-1963.68	

(continued)

Table 1. (continued)

	hERG	CYP3A4	P-gp
Telmisartan	-1577.13	-2680.13	-3372.02
Olmесartan	-1797.61	-1941.46	-2196.19
Enoxaparin	ND	ND	ND
Heparin	239.93	ND	-1331.20
Warfarin	-964.86	-1504.42	-1434.01
Apixaban	-2539.76	-3299.81	-2589.28
Dabigatran	-1643.52	-2483.90	-2656.35
Rivaroxaban	-2217.98	-3246.04	-3171.51
Edoxaban	-2368.58	-2836.16	-2943.56
Famotidine	-488.58	-737.46	-1014.68
Atorvastatin	-1848.12	-2537.29	-3055.77
Lovastatin	-2257.71	-3009.82	-3342.22
Rosuvastatin	-1474.64	-2289.92	-2934.73
Simvastatin	-2185.10	-2908.71	-3718.12
Pravastatin	-2111.09	-2874.94	-3459.53
Fluvastatin	-1330.39	-2290.86	-2800.67
Ivermectin	-1474.56	ND	ND
Niclosamide	-1498.97	-1613.18	-2105.60
Nitazoxanide	-1785.32	-1941.18	-2331.84
Ibuprofen	-890.62	-1200.48	-1535.20
Indomethacin	-1294.61	-1865.81	-2441.04
Alteplase	ND	ND	ND
Tenecteplase	ND	ND	ND

Net dG Bind

	0	to -500
	-500.01	to -1000
	-1000.01	to -1500
	-1500.01	to -2000
	-2000.01	to -3000
	-3000.01	to -3500
	ND	ND

ND = Not determined.

Pharmacodynamic interactions

Among the 47 pharmacodynamic DDIs between the repurposed COVID-19 drugs and antitubercular drugs identified from Micromedex, 31 interactions resulted in QT prolongation effects. These interactions were integrated with the free binding energy of the repurposed COVID-19 drugs and antitubercular drugs and their AZCERT classification in Table 2.

Chloroquine and hydroxychloroquine (HCQ) are known for their QT prolongation effect. The potency of these drugs towards inhibition of hERG was also established from the N.S of -1662.35 and -1803.59 for chloroquine and HCQ, respectively, by molecular modelling. However, ritonavir (N.S for hERG = -1298.24) and lopinavir (N.S for hERG = -1451.95) had a relatively lower binding with hERG (Table 1). The docking poses for chloroquine, HCQ, ritonavir and lopinavir in the hERG pocket are shown in Figure 2(a)–(d).

It has been reported previously that few fluoroquinolones are usually either substrates or inhibitors for P-gp.^{46–48} The N.S against P-gp for levofloxacin, moxifloxacin and ofloxacin are -1653.33 , -1470.86 and -1658.35 , respectively (Table 1). When these fluoroquinolones are co-administered with chloroquine, HCQ, ritonavir and lopinavir, which have a higher affinity for P-gp (Table 1), the elevated concentration of the later drugs could result in synergistic QT prolongation effects. The induced-fit docking poses of levofloxacin, moxifloxacin and ofloxacin with P-gp pocket are displayed in Figure 3(a)–(c).

Clofazimine is known to show a potent inhibitory effect on CYP3A4 *in vitro*.²⁵ The N.S of -2608.84 against CYP3A4 validates the claim. It is also a potent inhibitor of hERG.⁴⁹ The N.S of clofazimine against hERG and P-gp were found to be -2698.49 and -2943.46 , respectively (Table 1). The CYP3A4 and P-gp inhibitory effect of this drug would result in high levels of chloroquine, HCQ, ritonavir and lopinavir, thereby increasing the later drug's hERG inhibitory effect when co-administered. The fact that clofazimine itself binds to hERG strongly may also result in synergism with the other drugs. Besides these, we strongly suggest the possibility of simultaneous drug interactions in the hERG pocket. Our computational predictions assert that the hERG-drug

complexes are more stable with clofazimine when combined with another drug (chloroquine/HCQ/lopinavir/ritonavir/azithromycin/famotidine) than this or the other individual drugs being present in the pocket individually. The simultaneous docking poses are shown in Figure 4(a)–(f).

The DDI profile of delamanid is similar to that of clofazimine. Experimental data reports that it does not inhibit or induce CYP isoforms.⁵⁰ Therefore, inhibition of P-gp by delamanid (N.S = -2505.75) may be a strong reason that maybe attributed to the increased QT prolongation effect observed when it is co-administered with chloroquine, HCQ, ritonavir and lopinavir (Table 2). From the simultaneous docking study on the hERG pocket, we propose that delamanid may also interact very strongly (better than individual affinity) inside the hERG binding region with co-administered drugs like chloroquine, HCQ, ritonavir, lopinavir, azithromycin and famotidine (Table 2). If proven experimentally, the presence of two molecules inside the pocket and their high stability may establish new mechanisms in DDIs for QT prolongation. The simultaneous docking poses are shown in Figure 5(a)–(f).

Bedaquiline itself is a potent hERG inhibitor (N.S = -1717.55). Hence, it is expected to have a synergistic DDI with other QT prolonging drugs such as ritonavir, lopinavir, chloroquine and HCQ (Table 2). Our computational studies have shown a good binding score with CYP3A4 (N.S = -1597.47) and P-gp (N.S = -2141.56), which may be another possible reason for its synergistic effect on QT prolongation with the above drugs. Despite extensive IFD studies, we could not generate sufficient pose for azithromycin with hERG, CYP3A4 and P-gp pockets after docking. In the case of clarithromycin, molecular modelling data could not be generated due to the complexity of the mechanisms it exhibits. Famotidine also had a very low interaction with hERG protein (Table 1). Molecular modelling results have revealed that remdesivir (N.S = -1636.25) and streptomycin (N.S = -2137.80) had higher binding affinities towards hERG protein. Further clinical data is required to validate these modelling results.

We also identified 16 synergistic pharmacodynamic DDIs. Of these, 12 DDIs were between

Table 2. Pharmacodynamic DDIs resulting in QT prolongation, identified from Micromedex with the free binding energy and combination binding energy to hERG protein along with their AZCERT classification.

Drug 1	Free binding energy	Drug 2	Free binding energy	Binding free energy	MMGBSA dG Bind		
Repurposed COVID-19 drugs AZCERT classification		Antitubercular drugs AZCERT classification		Drug combinations			
Chloroquine ^a	-42.51	Levofloxacin ^a	-28.29	Levofloxacin + Chloroquine	-55.41		
				Chloroquine + Levofloxacin	-39.02		
		Moxifloxacin ^a	-22.76	Moxifloxacin + Chloroquine	-44.12		
				Chloroquine + Moxifloxacin	-24.41		
		Ofloxacin ^b	-28.29	Ofloxacin + Chloroquine	-55.41		
				Chloroquine + Ofloxacin	-39.02		
		Clarithromycin ^a	-28.22	Clarithromycin + Chloroquine	-32.94		
				Chloroquine + Clarithromycin	N.D.		
		Clofazimine ^b	-59.40	Clofazimine + Chloroquine	-59.31		
				Chloroquine + Clofazimine	-55.73		
		Delamanid ^b	-45.28	Delamanid + Chloroquine	-48.07		
				Chloroquine + Delamanid	-39.14		
		Bedaquiline ^b	-52.11	Bedaquiline + Chloroquine	-39.01		
				Chloroquine + Bedaquiline	-68.29		
		HCQ ^a	-53.40	Levofloxacin ^a	-28.29	Levofloxacin + HCQ	-60.21
						HCQ + Levofloxacin	-19.63
Moxifloxacin ^a	-22.76			Moxifloxacin + HCQ	-65.05		
				HCQ + Moxifloxacin	-40.44		
Ofloxacin ^b	-28.29			Ofloxacin + HCQ	-60.13		
				HCQ + Ofloxacin	-19.63		
Clarithromycin ^b	-28.22			Clarithromycin + HCQ	-40.17		
				HCQ + Clarithromycin	N.D.		
Clofazimine ^b	-59.40			Clofazimine + HCQ	-61.20		
				HCQ + Clofazimine	-86.57		
Delamanid ^b	45.28			Delamanid + HCQ	-60.91		
				HCQ + Delamanid	-42.92		
Bedaquiline ^b	-52.11			Bedaquiline + HCQ	-49.58		
				HCQ + Bedaquiline	-60.65		

(continued)

Table 2. (continued)

Drug 1		Drug 2		Binding free energy		
Lopinavir/Ritonavir ^b	-53.44/-59.19	Levofloxacin ^a	-28.29	Levofloxacin + Lopinavir	-52.83	
				Lopinavir + Levofloxacin	-35.17	
				Levofloxacin + Ritonavir	-63.80	
				Ritonavir + Levofloxacin	-25.08	
		Moxifloxacin ^a	-22.76	Moxifloxacin + Lopinavir:	-47.88	
				Lopinavir + Moxifloxacin	-36.38	
				Moxifloxacin + Ritonavir	-65.67	
				Ritonavir + Moxifloxacin	-30.89	
		Ofloxacin ^b	-28.29	Ofloxacin + Lopinavir	-52.83	
				Lopinavir + Ofloxacin	-26.19	
				Ofloxacin + Ritonavir	-63.80	
				Ritonavir + Ofloxacin	-25.08	
	Clarithromycin ^a	-28.22	Lopinavir + Clarithromycin	N.D.		
			Clarithromycin + Lopinavir	-55.53		
			Ritonavir + Clarithromycin	-25.33		
			Clarithromycin + Ritonavir	-40.20		
	Clofazimine ^b	-59.40	Clofazimine + Lopinavir	-72.86		
			Lopinavir + Clofazimine	-70.58		
			Clofazimine + Ritonavir	-57.87		
			Ritonavir + Clofazimine	-69.42		
	Delamanid ^b	-45.28	Delamanid + Lopinavir	-52.25		
			Lopinavir + Delamanid	-44.16		
			Delamanid + Ritonavir	-64.75		
			Ritonavir + Delamanid	-46.67		
Azithromycin ^a	-50.34	Levofloxacin ^b	-28.29	Levofloxacin + Azithromycin	-57.60	
				Azithromycin + Levofloxacin	-11.73	
		Moxifloxacin ^b	-22.76	Moxifloxacin + Azithromycin	-61.30	
				Azithromycin + Moxifloxacin	-30.10	
		Ofloxacin ^b	-28.29	Ofloxacin + Azithromycin	-73.31	
				Azithromycin + Ofloxacin	-11.73	
			Clarithromycin ^a	-28.22	Azithromycin + Clarithromycin	N.D.

(continued)

Table 2. (continued)

Drug 1	Drug 2	Binding free energy
		Clarithromycin + Azithromycin N.D.
	Clofazimine ^b -59.40	Clofazimine + Azithromycin -67.06
		Azithromycin + Clofazimine -43.18
	Delamanid ^b -45.28	Delamanid + Azithromycin -59.48
		Azithromycin + Delamanid -46.20
Famotidine ^c -16.12	Levofloxacin ^a -28.29	Levofloxacin + Famotidine -5.78
		Famotidine + Levofloxacin 2.96
	Clarithromycin ^a -28.22	Clarithromycin + Famotidine -7.42
		Famotidine + Clarithromycin -43.72
	Moxifloxacin ^a -22.76	Moxifloxacin + Famotidine -8.64
		Famotidine + Moxifloxacin -13.67
	Clofazimine ^b -59.40	Clofazimine + Famotidine N.D.
		Famotidine + Clofazimine -62.08
	Delamanid ^b -45.28	Delamanid + Famotidine N.D.
		Famotidine + Delamanid -50.33

AZCERT, Arizona Centre for Education and Research on Therapeutics; DDI, drug–drug interactions; HCQ, hydroxychloroquine; hERG, human Ether-à-go-go-Related Gene; N.D., not determined.

^aKnown risk of TdP.
^bPossible risk of TdP.
^cConditional risk of TdP.

corticosteroids (dexamethasone, hydrocortisone, methylprednisolone and budesonide) and fluoroquinolones (levofloxacin, moxifloxacin and ofloxacin) that could increase the risk of development of tendinopathy. The remaining 4 DDIs between non-steroidal anti-inflammatory drugs (NSAIDs; ibuprofen and indomethacin) with fluoroquinolones (levofloxacin and ofloxacin) could increase the risk of central nervous system stimulation and convulsive seizures.

Pharmacokinetic interactions

We identified a total of 42 pharmacokinetic DDIs between repurposed COVID-19 drugs and antitubercular drugs. The majority of these pharmacokinetic DDIs were explained by the ability of the antitubercular drugs and repurposed

COVID-19 drugs to inhibit or induce CYP3A4 and P-gp. This was further evidenced by computational studies as several drugs were found to be strong substrates of CYP3A4 and P-gp as shown in Table 1.

The first-line antitubercular drug rifampin was shown to interact with several drugs that were substrates of CYP3A4 and P-gp such as lopinavir/ritonavir, dexamethasone, hydrocortisone, methylprednisolone, ruxolitinib, losartan, apixaban, dabigatran, rivaroxaban, edoxaban and simvastatin. Clarithromycin also was found to pharmacokinetically interact with substrates of CYP3A4 and P-gp such as colchicine, dexamethasone, methylprednisolone, budesonide, ruxolitinib, calcifediol, losartan, warfarin, dabigatran, rivaroxaban, edoxaban, atorvastatin, lovastatin and simvastatin.

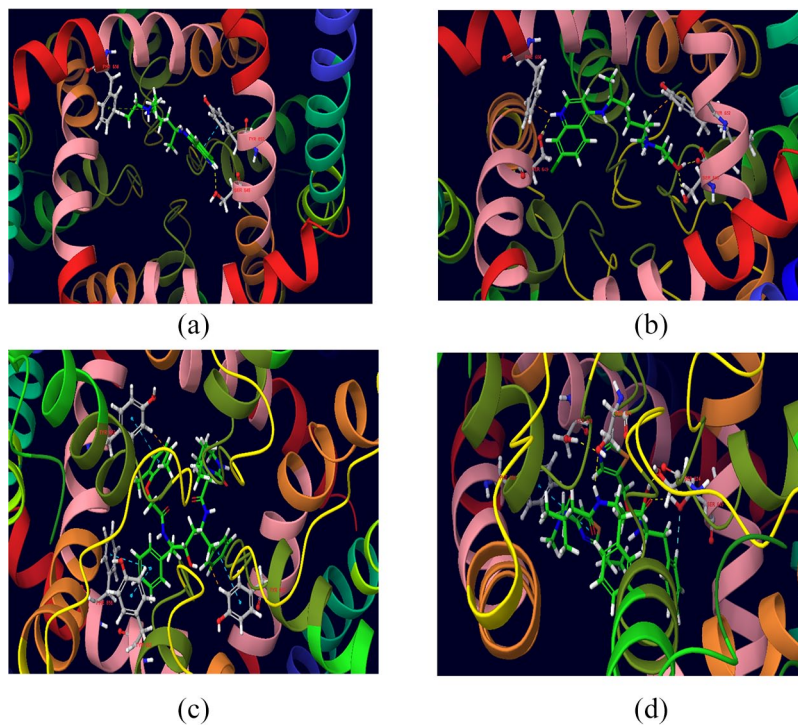


Figure 2. Docked pose of repurposed COVID-19 drugs: (a) chloroquine, (b) HCQ, (c) lopinavir and (d) ritonavir at hERG binding pocket.

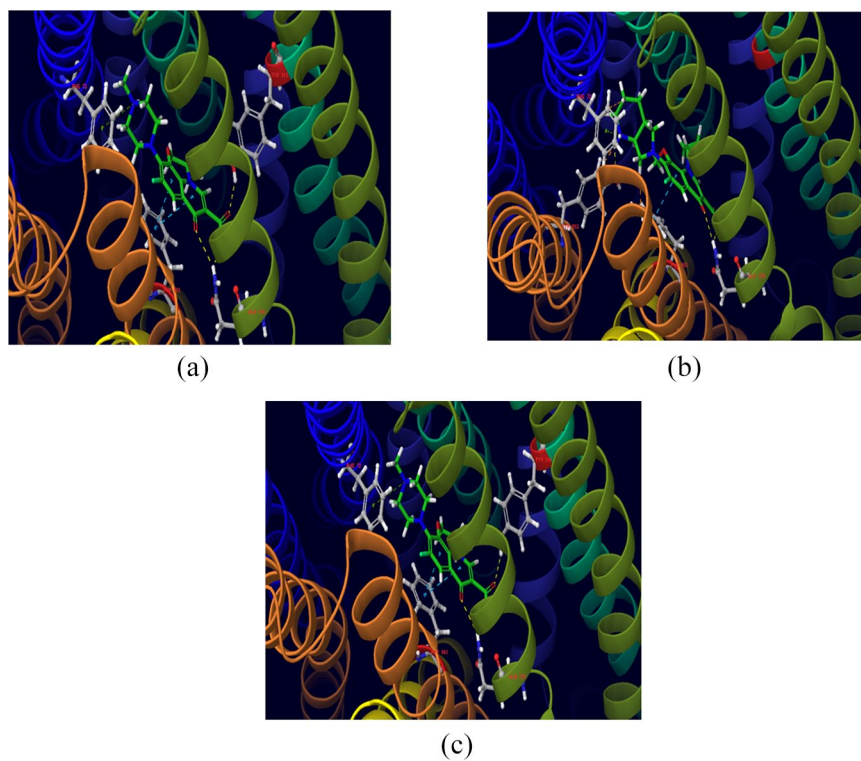


Figure 3. Docked pose of second-line antitubercular drugs, fluoroquinolones: (a) levofloxacin, (b) moxifloxacin and (c) ofloxacin at the P-gp binding pocket.

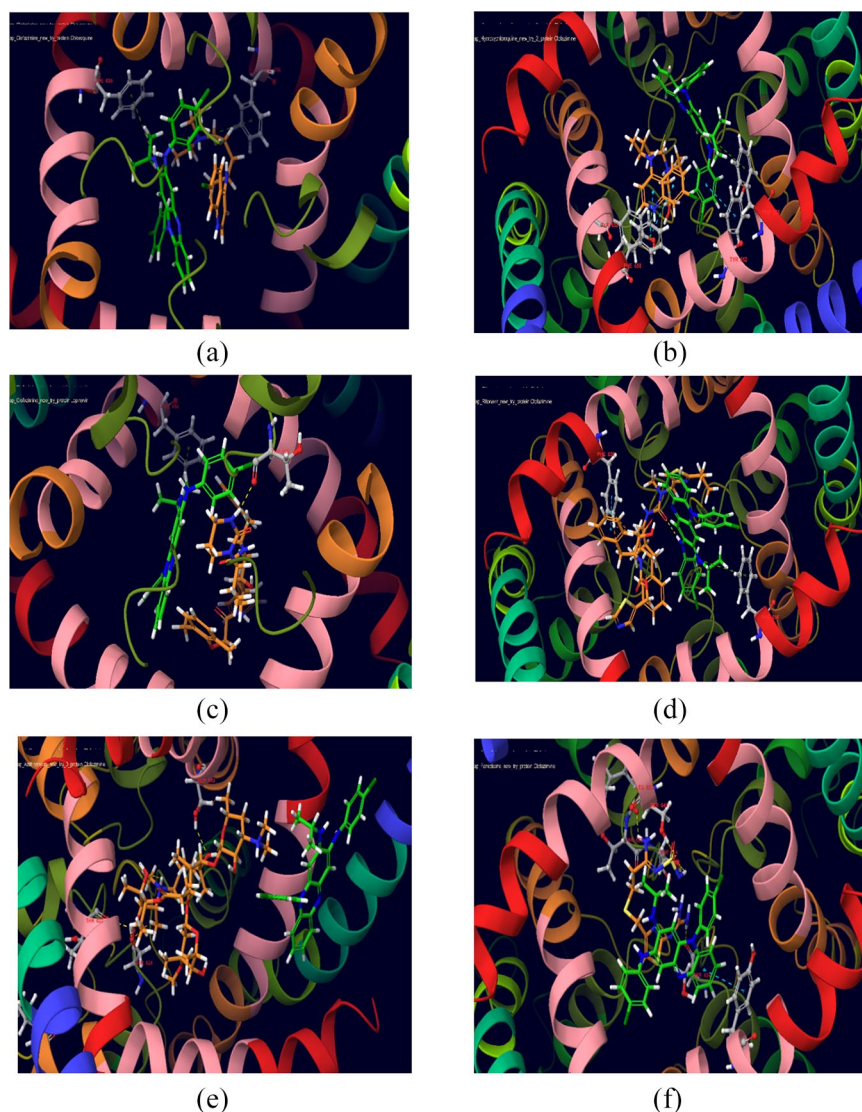


Figure 4. Simultaneous docking of clofazimine with (a) chloroquine, (b) HCQ, (c) lopinavir, (d) ritonavir, (e) azithromycin and (f) famotidine in hERG's binding pocket.

Computation studies have shown that hydrocortisone (N.S = -2377.34), methylprednisolone (N.S = -2832.10), colchicine (N.S = -2537.80), ruxolitinib (N.S = -2339.74), calcifediol (N.S = -3982.01), losartan (N.S = -2452.40), apixaban (N.S = -3299.81), dabigatran (N.S = -2483.90), rivaroxaban (N.S = -3246.04) and edoxaban (N.S = -2836.16) are strong substrates of CYP3A4. The induced-fit docking poses of lopinavir, ritonavir and apixaban with CYP3A4 pocket are displayed in Figure 6(a)–(c).

Ritonavir (N.S = -2095.04), hydrocortisone (N.S = -2846.07), methylprednisolone

(N.S = -2683.53), calcifediol (N.S = -3379.04), losartan (N.S = -2296.83), apixaban (N.S = -2589.28), dabigatran (N.S = -2656.35), rivaroxaban (N.S = -3171.51) and edoxaban (N.S = -2943.56) were found to be strong substrates of P-gp. The computational studies also indicate that remdesivir is an excellent substrate of P-gp (N.S = -2687.21) as shown in Figure 7(c). The induced-fit docking poses of ritonavir, hydrocortisone and remdesivir with P-gp pocket are displayed in Figure 7(a)–(c).

First-line antitubercular drugs like ethambutol and pyrazinamide as well as the second-line

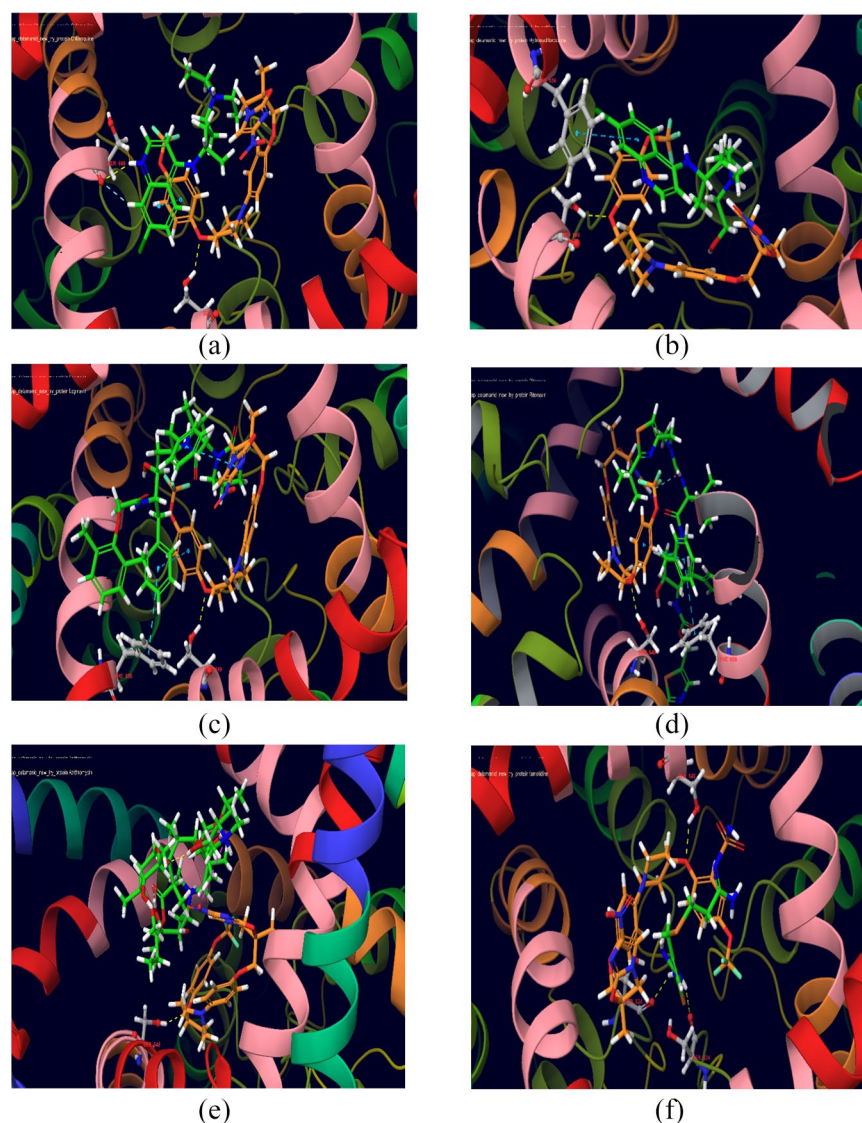


Figure 5. Simultaneous docking of delamanid with (a) chloroquine, (b) HCQ, (c) lopinavir, (d) ritonavir, (e) azithromycin and (f) famotidine in hERG's binding pocket.

drugs capreomycin, cycloserine, ethionamide, imipenem-cilastatin and pretomanid did not show any interactions with the repurposed COVID-19 drugs (Figure 1). These drugs had only weak-to-moderate binding with CYP3A4 and P-gp (Table 1).

Discussion

A large proportion of patients who develop active TB infection are immunocompromised.⁵¹ COVID-19 infection also possesses a perilous impact on the immune system.⁵² A synergy of

these two infections could result in severe menacing consequences.⁵³ COVID-19 co-infection with TB has been reported to worsen the prognosis and increase morbidity and mortality in patients affected with this dual infection.⁵⁴⁻⁵⁶ There is a sparsity of data regarding the number of patients who receive antitubercular as well as repurposed COVID-19 drugs simultaneously. Stochino and colleagues reported that 20 cases of COVID-19 infection were observed among 24 inpatients diagnosed with TB in a hospital setting in northern Italy. Among these 20 patients co-infected with COVID-19 and TB, drug sensitivity test results

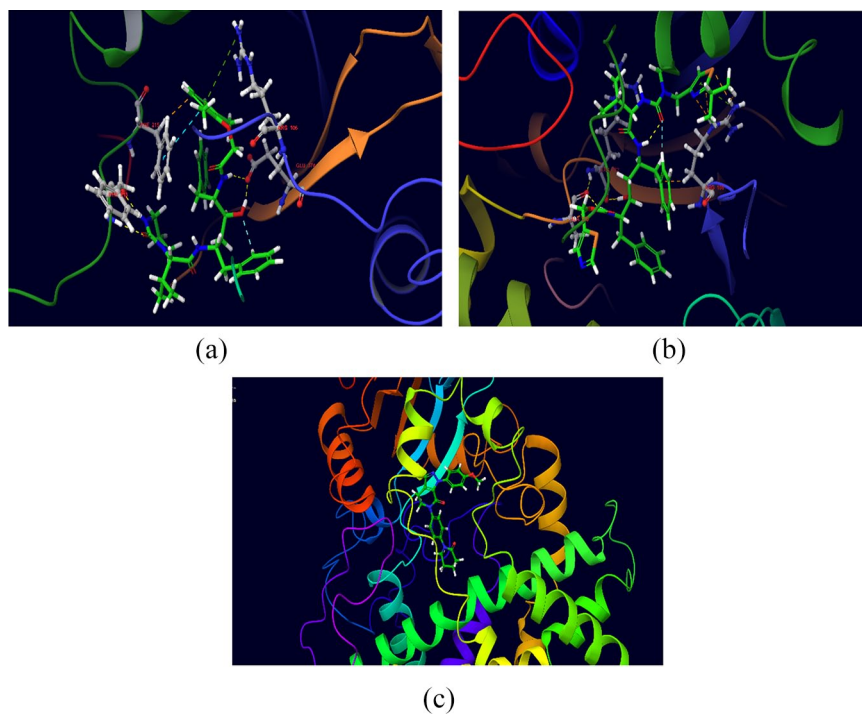


Figure 6. Docking pose of (a) lopinavir, (b) ritonavir and (c) apixaban at the CYP3A4 binding pocket.

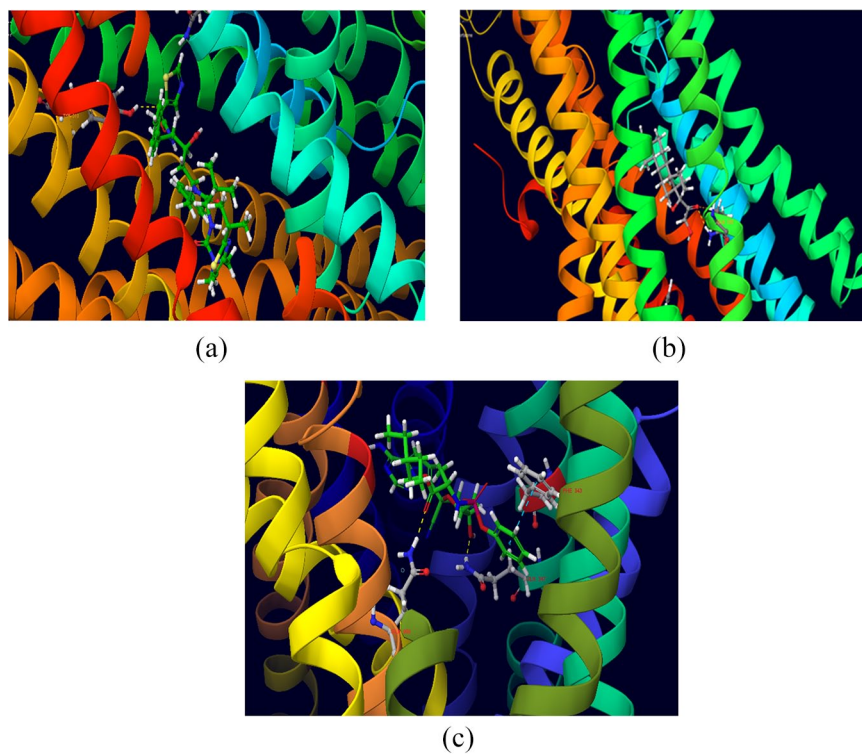


Figure 7. Docking pose of (a) ritonavir, (b) hydrocortisone and (c) remdesivir at the P-gp binding pocket.

showed that 3 patients were isoniazid resistant and 2 patients were multidrug-resistant. The standard first-line antitubercular treatment regimen was given in 14 cases, whereas a modified antitubercular regimen was given to 6 patients based on clinical characteristics and drug sensitivity test results. HCQ (200 mg twice a day) was administered to all TB patients co-infected with COVID-19 infection.⁵⁷ However, with the arrival of second and third wave of COVID-19 infection, there is a high potential for a significant population of TB patients to be infected with COVID-19 and vice versa, particularly in countries with a high TB burden. In this scenario, withholding the administration of antitubercular drugs is not a rational option as it has been reported that interruption of TB treatment is significantly associated with poor treatment outcomes and is one of the major hurdles associated with TB management, particularly of multidrug-resistant tuberculosis (MDR-TB).^{58–60} Hence, it is anticipated that in the coming days, there would be a significant proportion of TB patients who are likely to be co-infected with COVID-19 and could receive antitubercular as well as repurposed COVID-19 drugs simultaneously. Molecular docking is a widely used *in silico* method that aids in predicting interactions between molecules and biological targets.^{61,62} This is usually performed by first predicting the molecular orientation of a ligand within a receptor and then developing a scoring function based on IFD poses and energy calculations to estimate their complementarity.⁶¹ IFD incorporates the principle that ligand binding causes changes in the residue side chain conformations within the specified pocket, resulting in flexibility in the binding pocket of the receptor.⁶³ These tools are fundamentally based on molecular docking approach that has been demonstrated to be a potential tool in the study of drug interactions with hERG, CYP3A4 and P-gp.^{64–66} CYP3A4 has a broad ligand specificity and is involved in the metabolism of many drugs. Hence, inhibition/induction of CYP3A4 metabolic activity by one substrate can have a significant impact on the metabolism of other substrates.⁶⁷ Drugs that are inhibitors or inducers of P-gp could alter the pharmacokinetic profiles of co-administered drugs that are P-gp substrates, resulting in DDIs.^{68,69} The structure-assisted docking model has been reported to predict P-gp inhibition quite effectively.⁷⁰ There is a substantial overlap in drugs that interfere with CYP3A4 and P-gp. Dual P-gp

and CYP3A4 inhibitors, on the contrary, may not always have the same inhibitory potency against P-gp and CYP3A4.^{71,72} Hence, by studying the extent of binding of drugs with CYP3A4 and P-gp through docking studies could provide critical preliminary information about hERG, CYP3A4 and P-gp-mediated DDIs. We have explored the possibility of two drugs interacting in the same pocket, thereby causing better inhibitory effect on hERG than a single drug itself. Thereby, we propose a direct DDI with respect to hERG inhibition in many instances where the interactions are occurring independent of the metabolic enzymes. The DDIs reported in the current study through drug interaction checker and molecular modelling study are intended to aid clinicians in better management of COVID-19 and TB infection and should not impede the delivery of regular treatments for both the infections.

High costs involved in the new drug development process and concerns pertaining to production and distribution of COVID-19 vaccines have paved the way for instant ubiquity for repurposing the available drugs to manage COVID-19.^{73,74} TB patients develop poor medication adherence due to multiple factors such as poverty, lack of social support and food security, adverse drug effects and pill burden.⁷⁵ There is an anticipation of a higher incidence of COVID-19 infection among TB patients and vice versa, particularly in countries with a high TB burden. Therefore, a significant population would be expected to undergo repurposed COVID-19 drug therapy along with antitubercular therapy. Hence, it is very important to foresee and prevent or manage DDI in these patients to allay the development of poor TB and COVID-19 treatment outcomes. Changes in the expression and activity of transporters and drug metabolizing enzymes induced by the inflammatory response in COVID-19 infection could also possibly play a crucial role in developing DDIs.⁷⁶ Studies from Spain have reported a high frequency of DDIs identified between repurposed COVID-19 drugs and concomitant medications.^{77,78} Addition of corticosteroids in COVID-19 management resulted in a dramatic increase in the development of potential DDIs of class B (moderate DDIs: drug combinations requiring dose adjustment and drug concentration monitoring).⁷⁹ Recent studies have reported on the potential risk of developing QT prolongation, CYP450 and P-gp-based DDIs

between repurposed COVID-19 drugs and various drugs used for management of lung cancer, neuropsychiatric diseases, stroke, asthma and arrhythmia.^{16,17,80–82} We have identified several pharmacodynamic DDIs resulting in a potential risk of QT prolongation as well as CYP450 and P-gp-based pharmacokinetic DDIs between repurposed COVID-19 drugs and antitubercular drugs through Micromedex drug interaction checker. Most of the pharmacodynamic interactions were supported by the results of the molecular modelling data.

Pharmacodynamic interactions: Jain and colleagues reported that QT prolongation was prevalent among 19.65% ($n=103/524$) of the COVID-19 patients with electrocardiogram reports. Among these patients, 95.1% ($n=98$) of patients were on COVID-19-related QT-prolonging medications.⁸³ Chloroquine, HCQ, lopinavir, ritonavir, azithromycin and famotidine have been documented to cause QT prolongation.^{84–91} Concomitant use of azithromycin with HCQ caused a greater change in the QTc prolongation than HCQ alone.⁸⁶ Approximately 5% of patients who were on remdesivir therapy for COVID-19 had developed QT prolongation.⁸³ Several second-line antitubercular drugs such as clarithromycin, clofazimine, delamanid, levofloxacin, moxifloxacin, ofloxacin and bedaquiline are associated with QT prolongation.^{36,92–99} The hERG channel has been reported to interact with numerous drugs of widely varying structure, possibly due to the unusual shape of the ligand-binding site and its hydrophobic character. Several *in silico* approaches for predicting the blockade of hERG channel have been attempted.¹⁰⁰ Our molecular modelling study also found that the aminoglycosides given as second-line antitubercular drugs had higher affinity for binding with hERG pockets (Table 1). However, we did not find any DDIs related to the same in Micromedex. Therefore, it can be said that the induced fit docking study was not sufficient enough to explain these findings. We expect that analysis with more advanced studies like molecular dynamics simulation and further clinical studies investigating the QT prolongation potential of aminoglycosides are required to give conclusive evidence. Our findings show that several combinations of repurposed COVID-19 drugs with antitubercular drugs had a higher combination binding energy towards hERG.

Hence, concomitant administration of the repurposed COVID-19 drugs and antitubercular drugs can result in synergistic QT prolonging effects, which require vigilant monitoring. The majority of the identified DDIs from Micromedex, resulting in QT prolongation, were concordant with our molecular modelling results (Table 2). Further clinical studies are required to validate these data from patients who are co-infected with COVID-19 and TB. Necessary cautions should be taken to avoid QT prolongation arising as a DDI between these repurposed COVID-19 drugs and antitubercular drugs. Developing various early identification and management tools such as that of the Situation Background Assessment Recommendation (SBAR) and electronic registries for arrhythmias are some of the potential strategies that could be employed for screening and management of QT prolongation, especially in this co-infected situation.^{29,83} Concomitant use of the second-line antitubercular drugs such as fluoroquinolones (levofloxacin, moxifloxacin and ofloxacin) with corticosteroids such as dexamethasone, hydrocortisone, methylprednisolone can cause synergistic tendinopathy/tendon rupture, with a higher risk among females, patients aged above 60 years and long-term use of fluoroquinolones.^{101–104} Hence, corticosteroid therapy should be used with caution among MDR-TB patients taking fluoroquinolones. The concurrent administration of fluoroquinolones (levofloxacin and ofloxacin) with NSAIDs (ibuprofen and indomethacin) may increase the risk of central nervous system stimulation and convulsive seizures.^{105–107} Alternative therapy should be considered, especially in patients who are predisposed to seizure activity.

Pharmacokinetic interactions: The first-line antitubercular drug rifampin reduces the plasma concentration of several drugs such as lopinavir/ritonavir, dexamethasone, hydrocortisone, methylprednisolone, ruxolitinib, losartan, apixaban, dabigatran, rivaroxaban, edoxaban and simvastatin via indirect induction of CYP3A4 and P-gp. Rifampin binds to the pregnane X receptor (PXR) and constitutive androstane receptor (CAR) in the cytoplasm. It translocates into the nucleus to form a heterodimer with retinoic acid receptor RXR. Subsequently, the heterodimer binds to the promoter region of the target genes CYP3A4 and P-gp and activates the transcription of its open reading frame, leading to increased CYP3A4 and

P-gp expression.^{26,108} As CYP3A4 and P-gp are major pharmacokinetics determinants of lopinavir/ritonavir, dexamethasone, hydrocortisone, methylprednisolone, ruxolitinib, losartan, apixaban, dabigatran, rivaroxaban, edoxaban and simvastatin, CYP3A4 and P-gp induction could increase the metabolism of these drugs and consequently reduces its plasma concentration.^{109–123} Valsartan is a substrate of efflux transporters P-gp (N.S = -1861.07) and MRP (multidrug resistance-associated protein) and uptake transporter OATP (organic anion transporter polypeptide). Therefore, co-administration with rifampin, an inducer of all the above transporters, may increase valsartan exposure.¹²⁴ Concurrent use of atorvastatin and rifampin may result in decreased atorvastatin concentration when administered separately after rifampin or increased atorvastatin exposure when administered simultaneously with rifampin which is due to induction of CYP3A4 metabolism of atorvastatin by rifampin and inhibition of organic anion-transporting polypeptide (OATP1B1)-mediated atorvastatin hepatic reuptake by rifampin, respectively.^{125,126} Concurrent use of fluvastatin and rifampin may result in decreased fluvastatin effectiveness. Fluvastatin is a substrate for BCRP (intestinal), OATP1B1, OAT1B3, OAT2B1, CYP2C9 and CYP3A4. Fluvastatin interactions are predominantly related to complete inhibition of CYP2C9, and rifampin is a CYP2C9 inducer.^{127,128} Besides CYP3A4 and CYP2C9, rifampin is also an inducer of CYP1A2, CYP2C19 and CYP3A5.¹²⁹ Hence, concomitant administration of rifampin with warfarin that is metabolized by most of these CYP450 enzymes will result in an increased risk of bleeding. Another first-line antitubercular drug isoniazid could potentially inhibit a wide range of CYP450 enzymes such as CYP1A2, CYP2A6, CYP2C19, CYP3A4, CYP2C9 and CYP2E1.^{130,131} Warfarin molecule exist in 2 enantiomeric forms S- and R-warfarin. The S-warfarin is mainly metabolized by CYP2C9, whereas R-warfarin is mainly metabolized by CYP1A2 and CYP3A4.¹³² Isoniazid-mediated CYP450 enzyme inhibition will potentially result in elevation of the blood levels of warfarin, resulting in an increased tendency for bleeding when both the drugs are given concomitantly.

Bedaquiline is primarily metabolized in the liver by the CYP3A4 to a less active N-monodesmethyl metabolite, M2.¹³³ Hence,

concomitant administration of CYP3A4 inhibitors with bedaquiline could result in elevated plasma concentrations of bedaquiline, increasing the risk of toxicities such as QT prolongation.¹³⁴ Ritonavir, a high-affinity type II ligand binds irreversibly to CYP3A4 and inhibits it by multiple mechanisms. These include metabolic-intermediate complex formation, competitive inhibition, irreversible type II coordination to the heme iron, heme destruction and CYP3A4-mediated ritonavir activation and subsequently form a covalent bond to the apoprotein.^{135,136} The mechanism of DDI between clarithromycin and various drugs that are CYP3A4 substrates such as dexamethasone, methylprednisolone, budesonide, calcifediol, ruxolitinib, losartan, warfarin, atorvastatin, lovastatin and simvastatin is attributed to mechanism-based inhibition exerted by clarithromycin. CYP3A4 metabolizes clarithromycin to form reactive nitrosoalkane via N-demethylation. This reactive nitrosoalkane generated further interacts with CYP3A4 to form an intermediate metabolite complex. This metabolic intermediate covalently bonds to the same CYP3A4 enzyme and facilitates its inactivation. Hence, a larger dose of clarithromycin can result in more potent CYP3A4 inhibition because of the larger formation of metabolite intermediates that can further inhibit CYP3A4 activity.^{116,137–145} Concurrent use of clarithromycin and pravastatin may increase pravastatin exposure and an increased risk of myopathy or rhabdomyolysis by clarithromycin inhibiting in a concentration-dependent manner OATP1B1- and OATP1B3-mediated uptake of pravastatin.^{146,147} Clarithromycin could increase the plasma exposure of dabigatran and edoxaban by P-gp inhibition and rivaroxaban by P-gp as well as CYP3A4 inhibition resulting in an increased risk of bleeding.^{148–150} CYP3A4 plays a significant role in the metabolism of colchicine to its inactive metabolites. Colchicine is also a substrate for P-gp. Therefore, clarithromycin, through dual inhibition of CYP3A4 and P-gp, can increase the plasma concentrations of colchicine, resulting in the toxicity of the latter drug.¹⁵¹ Zinc chelates with fluoroquinolones such as levofloxacin, moxifloxacin and ofloxacin, resulting in significant reduction of their antimicrobial activity.^{152,153} Disruption of intestinal flora synthesizing vitamin K and inhibition of cytochrome P450 enzymes involved in the metabolism of warfarin are proposed to be the major mechanisms

involved in the drug interaction between antibiotics such as fluoroquinolones, amoxicillin-clavulanate and linezolid with warfarin resulting in increased risk of bleeding.^{154–156} Concurrent use of amikacin and indomethacin with ibuprofen may result in increased amikacin exposure. Changes in renal blood flow is postulated to be the mechanism involved in explaining the DDI between NSAIDs and aminoglycosides. Inhibition of renal prostaglandins by NSAIDs may affect the renal blood flow and glomerular filtration rate during the development of aminoglycoside nephrotoxicity.^{157–160} Ascorbic acid could reduce the antibacterial actions of streptomycin and kanamycin by mechanisms that are not fully understood.¹⁶¹ Since remdesivir was found to be an excellent substrate of P-gp (N.S = -2687.21) through modelling study, caution should be warranted when other P-gp inhibitors are given.

With the advent of pharmacogenomics, it becomes imperative to assess the potential impact of genetic polymorphisms of drug metabolizing enzymes and drug transporters to understand clinically critical DDIs. An interaction solely caused by drug response to CYP450 genetics is referred to as drug-gene interaction (DGI) whereas an interaction that is a cumulative effect of both a DDI and DGI is referred to as drug-drug-gene interaction (DDGI). The incorporation of gene variants of *CYP2D6*, *CYP2C19* and *CYP2C9* increased the number of potentially clinically significant interactions by ~51% in a retrospective analysis assessing drug interactions among 1143 patients.¹⁶² Since there is a significant proportion of DDIs explained by induction and inhibition of CYP3A4 enzyme and P-gp transporter in Figure 1, it may be useful in future to identify the influence of their genetic variants to predict potentially clinically significant interactions in especially patients who are on second-line antitubercular drugs such as clarithromycin or to understand rifampin-mediated DDIs. Single nucleotide polymorphisms (SNPs) in the *CYP3A4* could abolish, reduce or increase CYP3A4 enzymatic activity. The effect of SNPs in *CYP3A4* on substrate binding was found to be substrate specific.¹⁶³ The *ABCB1* or *MDR1* gene that encodes for P-gp is highly polymorphic and the allelic variants have been reported to significantly influence the P-gp transporter activity.¹⁶⁴ The distribution of certain *CYP3A4* and *MDR1* allelic variants appears to be ethnicity dependent.^{163,164} In these

contexts, assessing the influence of allelic variants of *CYP3A4* and *MDR1* on the pharmacokinetics of individual substrate as well as substrate combinations (identified to be interacting) will be required to establish the precise extent and risk of clinical consequences of DDIs in clinical scenarios in different ethnic populations.

Therefore, predicting potential DDIs related to CYP3A4, P-gp and hERG is crucial in delivering safe chemotherapeutic TB and COVID-19 care. Further computational methods such as molecular dynamic studies (MDS) and *in vitro* assessments would validate and refine the current research results, to scale up our findings into clinical practice. The authors will consider this in near future. The risks of DDIs identified in this study should not impede the delivery of repurposed COVID-19 drugs or antitubercular therapies in all situations. The proper precautions, monitoring and safety management could deter the adverse events arising from DDIs between these drugs in most scenarios. Summarizing these potential DDIs for clinical decision support is challenging. Further clinical data on the clinical significance of these DDIs are needed from well-designed pharmacokinetic/pharmacodynamic studies. This helps to validate the data coming from drug information databases and molecular docking studies. These data are required to rule out the possibilities of poor alert specificity and indiscriminate DDI warnings. However, the current study provides an initial thrust of alertness regarding the occurrence of possible DDIs between repurposed COVID-19 therapies and antitubercular therapies based on drug information software and molecular docking software data. This aids clinicians and medical researchers identify and predict DDIs, particularly in countries with increased incidences of TB and COVID-19 infections. DDI information generating from real-time clinical scenarios may be used to develop algorithms for managing DDIs in COVID-19 patients treated with antitubercular drugs and repurposed COVID-19 drugs. Physicians, pharmacists and other health care providers should be encouraged to report adverse drug reactions that occur while treating the co-infected patients to regional/zonal/national pharmacovigilance centres for the wide dissemination of the safety information. There is a need for a single open accessible DDIs repository that integrates the literature evidence

from *in silico*, *in vitro*, *in vivo* and real-time clinical data and provides health care providers with more precise and reliable information for clinical decision making.

Conclusion

The data derived from DDI checker software and *in silico* computational methods have predicted the possibility of several potential DDIs with repurposed COVID-19 drugs. This highlights the need for a conscientious treatment plan, particularly in MDR-TB patients. The great challenge is especially when repurposed COVID-19 drugs are co-administered with second-line antitubercular drugs with the potential for QT prolongation or with antitubercular drugs that are inducers or inhibitors of CYP3A4 and P-gp. Further clinical data from well-designed, real-time pharmacokinetic and pharmacodynamic research in the TB patients co-infected with COVID-19 is required for the pragmatic picture of the DDIs reported in this work. These integrated data could then be potentially employed by clinicians, pharmacists and other healthcare providers to develop a meticulous surveillance strategy to identify and manage the DDIs. This improves the treatment outcomes, reduces healthcare expenditures and decreases related morbidities and mortalities of the affected patients.

Acknowledgements

Levin Thomas, Sumit Raosaheb Birangal and Rajdeep Ray are thankful to Dr TMA Pai PhD Scholarship from Manipal Academy of Higher Education, Manipal, India. All the authors are thankful to Centre for Translational Research, MAHE and Manipal Schrodinger Centre for Molecular Simulations for providing computational facility to carry out the study. Levin Thomas and Sumit Raosaheb Birangal contributed equally.

Conflict of interest statement

The authors declared no potential conflicts of interest with respect to the research, authorship and/or publication of this article.

Ethical approval and consent to participate

No ethical approval was needed as this was an integrated data analysis from drug information database and *in silico* computational methods.

Funding

The authors received no financial support for the research, authorship and/or publication of this article.

ORCID iDs

Sonal Sekhar Miraj  <https://orcid.org/0000-0003-3660-2022>

Mahadev Rao  <https://orcid.org/0000-0003-3322-5399>

References

1. Ferkol T and Schraufnagel D. The global burden of respiratory disease. *Ann Am Thorac Soc* 2014; 11: 404–406.
2. World Health Organization. Global tuberculosis report 2020, <https://apps.who.int/iris/bitstream/handle/10665/336069/9789240013131-eng.pdf> (2020, accessed 5 November 2020).
3. Hallett T, Hogan A, Jewell B, *et al.* Potential impact of the COVID-19 pandemic on HIV, TB and malaria in low-and middle-income countries: a modelling study. *Lancet Glob Health* 2020; 8: e1132–e1141.
4. Stop TB Partnership. The potential impact of the COVID-19 response on tuberculosis in high-burden countries: a modelling analysis, http://www.stoptb.org/assets/documents/news/Modeling%20Report_1%20May%202020_FINAL.pdf (2020, accessed 2 November 2020).
5. Sumner A, Hoy C and Ortiz-Juarez E. *Estimates of the impact of COVID-19 on global poverty*. Helsinki: UNU-WIDER, 2020, pp. 1–14.
6. Carter DJ, Glaziou P, Lönnroth K, *et al.* The impact of social protection and poverty elimination on global tuberculosis incidence: a statistical modelling analysis of sustainable development goal 1. *Lancet Glob Health* 2018; 6: e514–e522.
7. Saunders MJ and Evans CA. COVID-19, tuberculosis, and poverty: preventing a perfect storm. *Eur Respir J* 2020; 56: 2001348.
8. Tamuzi JL, Ayele BT, Shumba CS, *et al.* Implications of COVID-19 in high burden countries for HIV/TB: a systematic review of evidence. *BMC Infect Dis* 2020; 20: 744.
9. Liu Y, Bi L, Chen Y, *et al.* Active or latent tuberculosis increases susceptibility to COVID-19 and disease severity. *medRxiv* 2020, <https://>

- www.medrxiv.org/content/10.1101/2020.03.10.20033795v1
10. Tadolini M, Codecasa LR, García-García JM, *et al.* Active tuberculosis, sequelae and COVID-19 co-infection: first cohort of 49 cases. *Eur Respir J* 2020; 56: 2001398.
 11. Mirošević Skvrce N, Macolić Šarinić V, Mucalo I, *et al.* Adverse drug reactions caused by drug-drug interactions reported to Croatian Agency for Medicinal Products and Medical Devices: a retrospective observational study. *Croat Med J* 2011; 52: 604–614.
 12. Khandeparkar A and Rataboli PV. A study of harmful drug–drug interactions due to polypharmacy in hospitalized patients in Goa Medical College. *Perspect Clin Res* 2017; 8: 180–186.
 13. Lazarou J, Pomeranz BH and Corey PN. Incidence of adverse drug reactions in hospitalized patients: a meta-analysis of prospective studies. *JAMA* 1998; 279: 1200–1205.
 14. Al-Arifi M, Abu-Hashem H, Al-Meziny M, *et al.* Emergency department visits and admissions due to drug related problems at Riyadh military hospital (RMH), Saudi Arabia. *Saudi Pharm J* 2014; 22: 17–25.
 15. Taylor R Jr, Pergolizzi JV Jr, Puenpatom RA, *et al.* Economic implications of potential drug–drug interactions in chronic pain patients. *Expert Rev Pharmacoecon Outcomes Res* 2013; 13: 725–734.
 16. Baburaj G, Thomas L and Rao M. Potential drug interactions of repurposed COVID-19 drugs with lung cancer pharmacotherapies. *Arch Med Res* 2021; 52: 261–269.
 17. Cattaneo D, Pasina L, Maggioni AP, *et al.* Drug–drug interactions and prescription appropriateness in patients with COVID-19: a retrospective analysis from a Reference Hospital in Northern Italy. *Drugs Aging* 2020; 37: 925–933.
 18. Roblek T, Vaupotic T, Mrhar A, *et al.* Drug-drug interaction software in clinical practice: a systematic review. *Eur J Clin Pharmacol* 2015; 71: 131–142.
 19. Kheshti R, Aalipour M and Namazi S. A comparison of five common drug–drug interaction software programs regarding accuracy and comprehensiveness. *J Res Pharm Pract* 2016; 5: 257–263.
 20. Safdari R, Ferdousi R, Aziziheris K, *et al.* Computerized techniques pave the way for drug-drug interaction prediction and interpretation. *Bioimpacts* 2016; 6: 71–78.
 21. Ferdousi R, Safdari R and Omidi Y. Computational prediction of drug-drug interactions based on drugs functional similarities. *J Biomed Inform* 2017; 70: 54–64.
 22. Sotgiu G, Centis R, D’ambrosio L, *et al.* Tuberculosis treatment and drug regimens. *Cold Spring Harb Perspect Med* 2015; 5: a017822.
 23. Ogu CC and Maxa JL. Drug interactions due to cytochrome P450. *Proc (Bayl Univ Med Cent)* 2000; 13: 421–423.
 24. Kim RB. Drugs as P-glycoprotein substrates, inhibitors, and inducers. *Drug Metab Rev* 2002; 34: 47–54.
 25. Horita Y and Doi N. Comparative study of the effects of antituberculosis drugs and antiretroviral drugs on cytochrome P450 3A4 and P-glycoprotein. *Antimicrob Agents Chemother* 2014; 58: 3168–3176.
 26. Chen J and Raymond K. Roles of rifampicin in drug-drug interactions: underlying molecular mechanisms involving the nuclear pregnane X receptor. *Ann Clin Microbiol Antimicrob* 2006; 5: 3.
 27. Guglielmetti L, Tiberi S, Burman M, *et al.* QT prolongation and cardiac toxicity of new tuberculosis drugs in Europe: a Tuberculosis Network European Trialsgroup (TBnet) study. *Eur Respir J* 2018; 52: 1800537.
 28. Harausz E, Cox H, Rich M, *et al.* QTc prolongation and treatment of multidrug-resistant tuberculosis. *Int J Tuberc Lung Dis* 2015; 19: 385–391.
 29. Crotti L and Arbelo E. COVID-19 treatments, QT interval and arrhythmic risk: the need for an international Registry on Arrhythmias. *Heart Rhythm* 2020; 17: 1423–1424.
 30. van den Broek MPH, Möhlmann JE, Abeln BGS, *et al.* Chloroquine-induced QTc prolongation in COVID-19 patients. *Neth Heart J* 2020; 28: 406–409.
 31. Vandenberg JI, Perry MD, Perrin MJ, *et al.* hERG K⁺ channels: structure, function, and clinical significance. *Physiol Rev* 2012; 92: 1393–1478.
 32. Gutman GA, Chandy KG, Adelman JP, *et al.* International Union of Pharmacology. XLI. Compendium of voltage-gated ion channels: potassium channels. *Pharmacol Rev* 2003; 55: 583–586.

33. Recanatini M, Poluzzi E, Masetti M, *et al.* QT prolongation through hERG K⁺ channel blockade: current knowledge and strategies for the early prediction during drug development. *Med Res Rev* 2005; 25: 133–166.
34. Hancox JC, McPate MJ, El Harchi A, *et al.* The hERG potassium channel and hERG screening for drug-induced torsades de pointes. *Pharmacol Ther* 2008; 119: 118–132.
35. Alexandrou AJ, Duncan RS, Sullivan A, *et al.* Mechanism of hERG K⁺ channel blockade by the fluoroquinolone antibiotic moxifloxacin. *Br J Pharmacol* 2006; 147: 905–916.
36. Briasoulis A, Agarwal V and Pierce WJ. QT prolongation and torsade de pointes induced by fluoroquinolones: infrequent side effects from commonly used medications. *Cardiology* 2011; 120: 103–110.
37. Goldstein EJ, Owens RC Jr and Nolin TD. Antimicrobial-associated QT interval prolongation: pointes of interest. *Clin Infect Dis* 2006; 43: 1603–1611.
38. Carpenter A, Chambers OJ, El Harchi A, *et al.* COVID-19 management and arrhythmia: risks and challenges for clinicians treating patients affected by SARS-CoV-2. *Front Cardiovasc Med* 2020; 7: 85.
39. American Society of Health-System Pharmacists. Assessment of evidence for COVID-19-related treatments, <https://www.ashp.org/-/media/8CA43C674C6D4335B6A19852843C4052.ashx> (accessed 23 March 2021).
40. RCSB PDB. <https://www.rcsb.org/> (accessed 10 November 2020).
41. Sevrioukova I. Interaction of human drug-metabolizing CYP3A4 with small inhibitory molecules. *Biochemistry* 2019; 58: 930–939.
42. Farid R, Day T, Friesner RA, *et al.* New insights about HERG blockade obtained from protein modeling, potential energy mapping, and docking studies. *Bioorg Med Chem* 2006; 14: 3160–3173.
43. Wan H, Selvaggio G and Pearlstein RA. Toward in vivo-relevant hERG safety assessment and mitigation strategies based on relationships between non-equilibrium blocker binding, three-dimensional channel-blocker interactions, dynamic occupancy, dynamic exposure, and cellular arrhythmia. *PLoS ONE* 2020; 15: e0234946.
44. Schwartz PJ and Woosley RL. Predicting the unpredictable: drug-induced QT prolongation and torsades de pointes. *J Am Coll Cardiol* 2016; 67: 1639–1650.
45. Woosley RL, Heise CW and Romero KA. QT drugs list, Crediblemeds.org (2016, accessed 20 November 2020).
46. Brillault J, De Castro WV, Harnois T, *et al.* P-glycoprotein-mediated transport of moxifloxacin in a Calu-3 lung epithelial cell model. *Antimicrob Agents Chemother* 2009; 53: 1457–1462.
47. Alvarez AI, Pérez M, Prieto JG, *et al.* Fluoroquinolone efflux mediated by ABC transporters. *J Pharm Sci* 2008; 97: 3483–3493.
48. Sood D, Kumar N, Singh A, *et al.* Antibacterial and pharmacological evaluation of fluoroquinolones: a chemoinformatics approach. *Genomics Inform* 2018; 16: 44–51.
49. Wallis RS. Cardiac safety of extensively drug-resistant tuberculosis regimens including bedaquiline, delamanid and clofazimine. *Eur Respir J* 2016; 48: 1526–1527.
50. Shimokawa Y, Sasahara K, Yoda N, *et al.* Delamanid does not inhibit or induce cytochrome p450 enzymes in vitro. *Biol Pharm Bull* 2014; 37: 1727–1735.
51. Roberts T, Beyers N, Aguirre A, *et al.* Immunosuppression during active tuberculosis is characterized by decreased interferon- γ production and CD25 expression with elevated forkhead box P3, transforming growth factor- β , and interleukin-4 mRNA levels. *J Infect Dis* 2007; 195: 870–878.
52. Shi Y, Wang Y, Shao C, *et al.* COVID-19 infection: the perspectives on immune responses. *Cell Death Differ* 2020; 27: 1451–1454.
53. Mousquer GT, Peres A and Fiegenbaum M. Pathology of TB/COVID-19 co-infection: the phantom menace. *Tuberculosis* 2021; 126: 102020.
54. Motta I, Centis R, D'Ambrosio L, *et al.* Tuberculosis, COVID-19 and migrants: preliminary analysis of deaths occurring in 69 patients from two cohorts. *Pulmonology* 2020; 26: 233–240.
55. Sy KTL, Haw NJL and Uy J. Previous and active tuberculosis increases risk of death and prolongs recovery in patients with COVID-19. *Infect Dis* 2020; 52: 902–907.
56. Davies MA. HIV and risk of COVID-19 death: a population cohort study from the Western Cape Province, South Africa. *medRxiv* 2020,

- <https://www.medrxiv.org/content/10.1101/2020.07.02.20145185v2.full>
57. Stochino C, Villa S, Zucchi P, *et al.* Clinical characteristics of COVID-19 and active tuberculosis co-infection in an Italian reference hospital. *Eur Respir J* 2020; 56: 2001708.
 58. Tola HH, Holakouie-Naieni K, Mansournia MA, *et al.* Intermittent treatment interruption and its effect on multidrug resistant tuberculosis treatment outcome in Ethiopia. *Sci Rep* 2019; 9: 20030.
 59. Jakubowiak W, Bogorodskaya E, Borisov S, *et al.* Treatment interruptions and duration associated with default among new patients with tuberculosis in six regions of Russia. *Int J Infect Dis* 2009; 13: 362–368.
 60. Bastard M, Sanchez-Padilla E, Hewison C, *et al.* Effects of treatment interruption patterns on treatment success among patients with multidrug-resistant tuberculosis in Armenia and Abkhazia. *J Infect Dis* 2015; 211: 1607–1615.
 61. Kitchen DB, Decornez H, Furr JR, *et al.* Docking and scoring in virtual screening for drug discovery: methods and applications. *Nat Rev Drug Discov* 2004; 3: 935–949.
 62. Pinzi L and Rastelli G. Molecular docking: shifting paradigms in drug discovery. *Int J Mol Sci* 2019; 20: 4331.
 63. Sotriffer CA. Accounting for induced-fit effects in docking: what is possible and what is not. *Curr Top Med Chem* 2011; 11: 179–191.
 64. Durdagi S, Randall T, Duff HJ, *et al.* Rehabilitating drug-induced long-QT promoters: in-silico design of hERG-neutral cisapride analogues with retained pharmacological activity. *BMC Pharmacol Toxicol* 2014; 15: 14.
 65. Lokwani DK, Sarkate AP, Karnik KS, *et al.* Structure-based site of metabolism (SOM) prediction of ligand for CYP3A4 enzyme: comparison of Glide XP and Induced Fit Docking (IFD). *Molecules* 2020; 25: 1622.
 66. Vilar S, Sobarzo-Sánchez E and Uriarte E. In silico prediction of P-glycoprotein binding: insights from molecular docking studies. *Curr Med Chem* 2019; 26: 1746–1760.
 67. Brown CM, Reisfeld B and Mayeno AN. Cytochromes P450: a structure-based summary of biotransformations using representative substrates. *Drug Metab Rev* 2008; 40: 1–100.
 68. Sugano K, Kansy M, Artursson P, *et al.* Coexistence of passive and carrier-mediated processes in drug transport. *Nat Rev Drug Discov* 2010; 9: 597–614.
 69. Elmeliogy M, Vourvahis M, Guo C, *et al.* Effect of P-glycoprotein (P-gp) inducers on exposure of P-gp substrates: review of clinical drug–drug interaction studies. *Clin Pharmacokinet* 2020; 59: 699–714.
 70. Klepsch F, Vasanathanathan P and Ecker GF. Ligand and structure-based classification models for prediction of P-glycoprotein inhibitors. *J Chem Inf Model* 2014; 54: 218–229.
 71. Wachter VJ, Wu CY and Benet LZ. Overlapping substrate specificities and tissue distribution of cytochrome P450 3A and P-glycoprotein: implications for drug delivery and activity in cancer chemotherapy. *Mol Carcinog* 1995; 13: 129–134.
 72. Lund M, Petersen TS and Dalhoff KP. Clinical implications of P-glycoprotein modulation in drug–drug interactions. *Drugs* 2017; 77: 859–883.
 73. Singh TU, Parida S, Lingaraju MC, *et al.* Drug repurposing approach to fight COVID-19. *Pharmacol Rep* 2020; 72: 1479–1508.
 74. Forni G, Mantovani A and COVID-19 Commission of Accademia Nazionale dei Lincei Rome. COVID-19 vaccines: where we stand and challenges ahead. *Cell Death Differ* 2021; 28: 626–639.
 75. Gugssa Boru C, Shimels T and Bilal AI. Factors contributing to non-adherence with treatment among TB patients in Sodo Woreda, Gurage Zone, Southern Ethiopia: a qualitative study. *J Infect Public Health* 2017; 10: 527–533.
 76. Kumar D and Trivedi N. Disease-drug and drug-drug interaction in COVID-19: risk and assessment. *Biomed Pharmacother* 2021; 139: 111642.
 77. Macías J, Pinilla A, Lao-Dominguez FA, *et al.* High rate of major drug–drug interactions of lopinavir–ritonavir for COVID-19 treatment. *Sci Rep* 2020; 10: 20958.
 78. Cantudo-Cuenca M, Gutiérrez-Pizarra A, Pinilla-Fernández A, *et al.* Drug–drug interactions between treatment specific pharmacotherapy and concomitant medication in patients with COVID-19 in the first wave in Spain. *Sci Rep* 2021; 11: 12414.
 79. Cattaneo D, Pasina L, Conti F, *et al.* Risks of potential drug–drug interactions in COVID-19

- patients treated with corticosteroids: a single-center experience. *J Endocrinol Invest*. Epub ahead of print 30 May 2021. DOI: 10.1007/s40618-021-01604-6.
80. Plasencia-García BO, Rodríguez-Menéndez G, Rico-Rangel MI, *et al*. Drug-drug interactions between COVID-19 treatments and antipsychotics drugs: integrated evidence from 4 databases and a systematic review. *Psychopharmacology* 2021; 238: 329–340.
 81. Bishara D, Kalafatis C and Taylor D. Emerging and experimental treatments for COVID-19 and drug interactions with psychotropic agents. *Ther Adv Psychopharmacol* 2020; 10: 2045125320935306.
 82. Ghasemiyeh P, Borhani-Haghighi A, Karimzadeh I, *et al*. Major neurologic adverse drug reactions, potential drug–drug interactions and pharmacokinetic aspects of drugs used in COVID-19 patients with stroke: a narrative review. *Ther Clin Risk Manag* 2020; 16: 595–605.
 83. Jain S, Workman V, Ganeshan R, *et al*. Enhanced electrocardiographic monitoring of patients with coronavirus disease 2019. *Heart Rhythm* 2020; 17: 1417–1422.
 84. Bustos M, Gay F, Diquet B, *et al*. The pharmacokinetics and electrocardiographic effects of chloroquine in healthy subjects. *Trop Med Parasitol* 1994; 45: 83–86.
 85. Khobragade SB, Gupta P, Gurav P, *et al*. Assessment of proarrhythmic activity of chloroquine in in vivo and ex vivo rabbit models. *J Pharmacol Pharmacother* 2013; 4: 116–124.
 86. Mercurio NJ, Yen CF, Shim DJ, *et al*. Risk of QT interval prolongation associated with use of hydroxychloroquine with or without concomitant azithromycin among hospitalized patients testing positive for coronavirus disease 2019 (COVID-19). *JAMA Cardiol* 2020; 5: 1036–1041.
 87. Anson BD, Weaver JG, Ackerman MJ, *et al*. Blockade of HERG channels by HIV protease inhibitors. *Lancet* 2005; 365: 682–686.
 88. Choi Y, Lim HS, Chung D, *et al*. Risk evaluation of azithromycin-induced QT prolongation in real-world practice. *Biomed Res Int* 2018; 2018: 1574806.
 89. Yun J, Hwangbo E, Lee J, *et al*. Analysis of an ECG record database reveals QT interval prolongation potential of famotidine in a large Korean population. *Cardiovasc Toxicol* 2015; 15: 197–202.
 90. Lee KW, Kayser SR, Hongo RH, *et al*. Famotidine and long QT syndrome. *Am J Cardiol* 2004; 93: 1325–1327.
 91. Endo T, Katoh T, Kiuchi K, *et al*. Famotidine and acquired long QT syndrome. *Am J Med* 2000; 108: 438–439.
 92. Svanström H, Pasternak B and Hviid A. Use of clarithromycin and roxithromycin and risk of cardiac death: cohort study. *BMJ* 2014; 349: g4930.
 93. Cetin M, Yıldırım M, Özen S, *et al*. Clarithromycin-induced long QT syndrome: a case report. *Case Rep Med* 2012; 2012: 634652.
 94. Yoon H, Jo K, Nam G, *et al*. Clinical significance of QT-prolonging drug use in patients with MDR-TB or NTM disease. *Int J Tuberc Lung Dis* 2017; 21: 996–1001.
 95. Gupta R, Geiter LJ, Hafkin J, *et al*. Delamanid and QT prolongation in the treatment of multidrug-resistant tuberculosis. *Int J Tuberc Lung Dis* 2015; 19: 1261–1262.
 96. Kervezee L, Gotta V, Stevens J, *et al*. Levofloxacin-induced QTc prolongation depends on the time of drug administration. *CPT Pharmacometrics Syst Pharmacol* 2016; 5: 466–474.
 97. Haverkamp W, Kruesmann F, Fritsch A, *et al*. Update on the cardiac safety of moxifloxacin. *Curr Drug Saf* 2012; 7: 149–163.
 98. Pontali E, Sotgiu G, Tiberi S, *et al*. Cardiac safety of bedaquiline: a systematic and critical analysis of the evidence. *Eur Respir J* 2017; 50: 1701462.
 99. Frommeyer G and Eckardt L. Drug-induced proarrhythmia: risk factors and electrophysiological mechanisms. *Nat Rev Cardiol* 2016; 13: 36–47.
 100. Aronov AM. Predictive in silico modeling for hERG channel blockers. *Drug Discov Today* 2005; 10: 149–155.
 101. Sendzik J, Shakibaei M, Schäfer-Korting M, *et al*. Synergistic effects of dexamethasone and quinolones on human-derived tendon cells. *Int J Antimicrob Agents* 2010; 35: 366–374.
 102. Persson R and Jick S. Clinical implications of the association between fluoroquinolones and tendon rupture: the magnitude of the effect with and without corticosteroids. *Br J Clin Pharmacol* 2019; 85: 949–959.
 103. Morales DR, Slattery J, Pacurariu A, *et al*. Relative and absolute risk of tendon rupture

- with fluoroquinolone and concomitant fluoroquinolone/corticosteroid therapy: population-based nested case-control study. *Clin Drug Investig* 2019; 39: 205–213.
104. Leone R, Magro L, Moretti U, *et al.* Identifying adverse drug reactions associated with drug-drug interactions. *Drug Saf* 2010; 33: 667–675.
 105. Hori S, Kizu J and Kawamura M. Effects of anti-inflammatory drugs on convulsant activity of quinolones: a comparative study of drug interaction between quinolones and anti-inflammatory drugs. *J Infect Chemother* 2003; 9: 314–320.
 106. Davey P. Overview of drug interactions with the quinolones. *J Antimicrob Chemother* 1988; 22(Suppl. C): 97–107.
 107. Ball P and Tillotson G. Tolerability of fluoroquinolone antibiotics. *Drug Saf* 1995; 13: 343–358.
 108. Chang HY, Chen CJ, Ma WC, *et al.* Modulation of pregnane X receptor (PXR) and constitutive androstane receptor (CAR) activation by ursolic acid (UA) attenuates rifampin-isoniazid cytotoxicity. *Phytomedicine* 2017; 36: 37–49.
 109. Tomlinson E, Maggs J, Park B, *et al.* Dexamethasone metabolism in vitro: species differences. *J Steroid Biochem Mol Biol* 1997; 62: 345–352.
 110. Zhang Y, Lu M, Sun X, *et al.* Expression and activity of p-glycoprotein elevated by dexamethasone in cultured retinal pigment epithelium involve glucocorticoid receptor and pregnane X receptor. *Invest Ophthalmol Vis Sci* 2012; 53: 3508–3515.
 111. van Waterschoot RA, ter Heine R, Wagenaar E, *et al.* Effects of cytochrome P450 3A (CYP3A) and the drug transporters P-glycoprotein (MDR1/ABCB1) and MRP2 (ABCC2) on the pharmacokinetics of lopinavir. *Br J Pharmacol* 2010; 160: 1224–1233.
 112. Stolbach A, Paziana K, Heverling H, *et al.* A review of the toxicity of HIV medications II: interactions with drugs and complementary and alternative medicine products. *J Med Toxicol* 2015; 11: 326–341.
 113. Thijs E, Wierckx K, Vandecasteele S, *et al.* Adrenal insufficiency, be aware of drug interactions! *Endocrinol Diabetes Metab Case Rep* 2019; 2019: 19-0062.
 114. Buffington GA, Dominguez JH, Piering WF, *et al.* Interaction of rifampin and glucocorticoids: adverse effect on renal allograft function. *JAMA* 1976; 236: 1958–1960.
 115. Branco B, Metsu D, Dutertre M, *et al.* Use of rifampin for treatment of disseminated tuberculosis in a patient with primary myelofibrosis on ruxolitinib. *Ann Hematol* 2016; 95: 1207–1209.
 116. Umehara K, Huth F, Jin Y, *et al.* Drug-drug interaction (DDI) assessments of ruxolitinib, a dual substrate of CYP3A4 and CYP2C9, using a verified physiologically based pharmacokinetic (PBPK) model to support regulatory submissions. *Drug Metab Pers Ther* 2019; 34: 20180042.
 117. Williamson KM, Patterson JH, McQueen RH, *et al.* Effects of erythromycin or rifampin on losartan pharmacokinetics in healthy volunteers. *Clin Pharmacol Ther* 1998; 63: 316–323.
 118. Sica DA, Gehr TW and Ghosh S. Clinical pharmacokinetics of losartan. *Clin Pharmacokinet* 2005; 44: 797–814.
 119. Vakkalagadda B, Frost C, Byon W, *et al.* Effect of rifampin on the pharmacokinetics of apixaban, an oral direct inhibitor of factor Xa. *Am J Cardiovasc Drugs* 2016; 16: 119–127.
 120. Hager N, Bolt J, Albers L, *et al.* Development of left atrial thrombus after coadministration of dabigatran etexilate and phenytoin. *Can J Cardiol* 2017; 33: 554.e13–554.e14.
 121. Forbes HL and Polasek TM. Potential drug-drug interactions with direct oral anticoagulants in elderly hospitalized patients. *Ther Adv Drug Saf* 2017; 8: 319–328.
 122. Mendell J, Chen S, He L, *et al.* The effect of rifampin on the pharmacokinetics of edoxaban in healthy adults. *Clin Drug Investig* 2015; 35: 447–453.
 123. Kyrklund C, Backman JT, Kivistö KT, *et al.* Rifampin greatly reduces plasma simvastatin and simvastatin acid concentrations. *Clin Pharmacol Ther* 2000; 68: 592–597.
 124. Liu W, Yan T, Chen K, *et al.* Predicting interactions between rifampin and antihypertensive drugs using the Biopharmaceutics Drug Disposition Classification System. *Pharmacotherapy* 2020; 40: 274–290.
 125. Backman JT, Luurila H, Neuvonen M, *et al.* Rifampin markedly decreases and gemfibrozil increases the plasma concentrations of atorvastatin and its metabolites. *Clin Pharmacol Ther* 2005; 78: 154–167.

126. Lau Y, Huang Y, Frassetto L, *et al.* Effect of OATP1B transporter inhibition on the pharmacokinetics of atorvastatin in healthy volunteers. *Clin Pharmacol Ther* 2007; 81: 194–204.
127. Kellick KA, Bottorff M, Toth PP, *et al.* A clinician's guide to statin drug-drug interactions. *J Clin Lipidol* 2014; 8(Suppl. 3): S30–S46.
128. Chen Y, Ferguson SS, Negishi M, *et al.* Induction of human CYP2C9 by rifampicin, hyperforin, and phenobarbital is mediated by the pregnane X receptor. *J Pharmacol Exp Ther* 2004; 308: 495–501.
129. Lynch T and Price AL. The effect of cytochrome P450 metabolism on drug response, interactions, and adverse effects. *Am Fam Physician* 2007; 76: 391–396.
130. Self TH, Chrisman CR, Baciewicz AM, *et al.* Isoniazid drug and food interactions. *Am J Med Sci* 1999; 317: 304–311.
131. Nishimura Y, Kurata N, Sakurai E, *et al.* Inhibitory effect of antituberculosis drugs on human cytochrome P450-mediated activities. *J Pharmacol Sci* 2004; 96: 293–300.
132. Kaminsky LS and Zhang ZY. Human P450 metabolism of warfarin. *Pharmacol Ther* 1997; 73: 67–74.
133. van Heeswijk RP, Dannemann B and Hoetelmans RM. Bedaquiline: a review of human pharmacokinetics and drug–drug interactions. *J Antimicrob Chemother* 2014; 69: 2310–2318.
134. Diacon AH, Pym A, Grobusch MP, *et al.* Multidrug-resistant tuberculosis and culture conversion with bedaquiline. *N Engl J Med* 2014; 371: 723–732.
135. Sevrioukova IF and Poulos TL. Structure and mechanism of the complex between cytochrome P4503A4 and ritonavir. *Proc Natl Acad Sci USA* 2010; 107: 18422–18427.
136. Rock BM, Hengel SM, Rock DA, *et al.* Characterization of ritonavir-mediated inactivation of cytochrome P450 3A4. *Mol Pharmacol* 2014; 86: 665–674.
137. Zhou S, Yung Chan S, Cher Goh B, *et al.* Mechanism-based inhibition of cytochrome P450 3A4 by therapeutic drugs. *Clin Pharmacokinet* 2005; 44: 279–304.
138. Tinel M, Descatoire V, Larrey D, *et al.* Effects of clarithromycin on cytochrome P-450. *J Pharmacol Exp Ther* 1989; 250: 746–751.
139. Delaforge M, Jaouen M and Mansuy D. Dual effects of macrolide antibiotics on rat liver cytochrome P-450: induction and formation of metabolite-complexes: a structure–activity relationship. *Biochem Pharmacol* 1983; 32: 2309–2318.
140. Mayhew BS, Jones DR and Hall SD. An in vitro model for predicting in vivo inhibition of cytochrome P450 3A4 by metabolic intermediate complex formation. *Drug Metab Dispos* 2000; 28: 1031–1037.
141. Wang Z, Lin YS, Dickmann LJ, *et al.* Enhancement of hepatic 4-hydroxylation of 25-hydroxyvitamin D3 through CYP3A4 induction in vitro and in vivo: implications for drug-induced osteomalacia. *J Bone Miner Res* 2013; 28: 1101–1116.
142. Recker MW and Kier KL. Potential interaction between clarithromycin and warfarin. *Ann Pharmacother* 1997; 31: 996–998.
143. Amsden GW, Kuye O and Wei GC. A study of the interaction potential of azithromycin and clarithromycin with atorvastatin in healthy volunteers. *J Clin Pharmacol* 2002; 42: 444–449.
144. Patel AM, Shariff S, Bailey DG, *et al.* Statin toxicity from macrolide antibiotic coprescription: a population-based cohort study. *Ann Intern Med* 2013; 158: 869–876.
145. Lee AJ and Maddix DS. Rhabdomyolysis secondary to a drug interaction between simvastatin and clarithromycin. *Ann Pharmacother* 2001; 35: 26–31.
146. Li DQ, Kim R, McArthur E, *et al.* Risk of adverse events among older adults following co-prescription of clarithromycin and statins not metabolized by cytochrome P450 3A4. *CMAJ* 2015; 187: 174–180.
147. Seithel A, Eberl S, Singer K, *et al.* The influence of macrolide antibiotics on the uptake of organic anions and drugs mediated by OATP1B1 and OATP1B3. *Drug Metab Dispos* 2007; 35: 779–786.
148. Delavenne X, Ollier E, Basset T, *et al.* A semi-mechanistic absorption model to evaluate drug–drug interaction with dabigatran: application with clarithromycin. *Br J Clin Pharmacol* 2013; 76: 107–113.
149. Mueck W, Kubitza D and Becka M. Co-administration of rivaroxaban with drugs that share its elimination pathways: pharmacokinetic effects in healthy subjects. *Br J Clin Pharmacol* 2013; 76: 455–466.

150. Corsini A, Ferri N, Proietti M, *et al.* Edoxaban and the Issue of drug-drug interactions: from pharmacology to clinical practice. *Drugs* 2020; 80: 1065–1083.
151. Ben-Chetrit E. Colchicine. In: Hashkes PJ, Laxer RM and Simon A (eds) *Textbook of autoinflammation*. Cham: Springer, 2019, pp. 729–749.
152. Seedher N and Agarwal P. Effect of metal ions on some pharmacologically relevant interactions involving fluoroquinolone antibiotics. *Drug Metabol Drug Interact* 2010; 25: 17–24.
153. Lomaestro BM and Bailie GR. Absorption interactions with fluoroquinolones. *Drug Saf* 1995; 12: 314–333.
154. Baillargeon J, Holmes HM, Lin YL, *et al.* Concurrent use of warfarin and antibiotics and the risk of bleeding in older adults. *Am J Med* 2012; 125: 183–189.
155. Lane MA, Zeringue A and McDonald JR. Serious bleeding events due to warfarin and antibiotic co-prescription in a cohort of veterans. *Am J Med* 2014; 127: 657–663.e2.
156. Sakai Y, Naito T, Arima C, *et al.* Potential drug interaction between warfarin and linezolid. *Intern Med* 2015; 54: 459–464.
157. Allegaert K, Cossey V, Langhendries J, *et al.* Effects of co-administration of ibuprofen-lysine on the pharmacokinetics of amikacin in preterm infants during the first days of life. *Biol Neonate* 2004; 86: 207–211.
158. Kovesi TA, Swartz R and MacDonald N. Transient renal failure due to simultaneous ibuprofen and aminoglycoside therapy in children with cystic fibrosis. *N Engl J Med* 1998; 338: 65–66.
159. Assael B, Chiabrando C, Gagliardi L, *et al.* Prostaglandins and aminoglycoside nephrotoxicity. *Toxicol Appl Pharmacol* 1985; 78: 386–394.
160. Clive DM and Stoff JS. Renal syndromes associated with nonsteroidal antiinflammatory drugs. *N Engl J Med* 1984; 310: 563–572.
161. Goswami M, Mangoli SH and Jawali N. Effects of glutathione and ascorbic acid on streptomycin sensitivity of *Escherichia coli*. *Antimicrob Agents Chemother* 2007; 51: 1119–1122.
162. Verbeurgt P, Mamiya T and Oesterheld J. How common are drug and gene interactions? Prevalence in a sample of 1143 patients with CYP2C9, CYP2C19 and CYP2D6 genotyping. *Pharmacogenomics* 2014; 15: 655–665.
163. Guttman Y, Nudel A and Kerem Z. Polymorphism in cytochrome P450 3A4 is ethnicity related. *Front Genet* 2019; 10: 224.
164. Ahmed S, Zhou Z, Zhou J, *et al.* Pharmacogenomics of drug metabolizing enzymes and transporters: relevance to precision medicine. *Genomics Proteomics Bioinformatics* 2016; 14: 298–313.

Visit SAGE journals online
[journals.sagepub.com/
 home/taw](http://journals.sagepub.com/home/taw)

 SAGE journals